Nutrient processing domains: Spatial and temporal patterns of material retention in running waters

H. Maurice Valett[1,4], Marc Peipoch[1,2,5], and Geoffrey C. Poole[3,6]

[1]Division of Biological Sciences, 32 Campus Drive, University of Montana, Missoula, Montana 59812 USA
[2]Stroud Water Research Center, 970 Spencer Road, Avondale, Pennsylvania 19311 USA
[3]Department of Land Resources and Environmental Sciences, 334 Leon Johnson Hall, P.O. Box 173120, Montana State University, Bozeman, Montana 59717 USA

Abstract: Reaches are a fundamental unit for lotic biogeochemical characterization, yet a functional classification of nutrient processing at the reach scale is currently lacking. Here, we introduce nutrient processing domains (NPDs) to integrate routing (nutrient delivery) and local (benthic uptake and transformation) processes that dictate longitudinal patterns of lotic biogeochemical function. An NPD is defined as a realm in functional space occupied by reaches that share similar biogeochemical character. Occupation of a given NPD reflects characteristic net material balance (NMB), exchange potential, and availability, associated with changes in solute load, the extent of hydrologic gain or loss, and changes in concentration from the head to the base of a reach, respectively. Using a mass-balance approach, we represent NMB as the effective solute flux (F_{eff}, M L^{-2} T^{-1}, where M = mass, L = length, and T = time), designating reaches as sources ($+F_{\mathrm{eff}}$) or sinks ($-F_{\mathrm{eff}}$). Discharge change along a reach is measured as the change in hydraulic load (ΔH_L, L/T), reflecting the potential for import and export to influence solute loads. Finally, the ratio of downstream-to-upstream concentration ($C_{\mathrm{dwn:up}}$) represents the net effect that processes have on nutrient availability. Using a 20-y historical record for N and P in the Upper Clark Fork River, Montana, USA, we employed this approach to 3 consecutive reaches covering nearly 90 km of channel length to address spatial and temporal dynamics in NPD behavior in a nutrient-rich, productive river system. For total N and total P, reaches typically occupied compiler or enhancer NPDs, displaying load increases without or with concomitant increases in concentration, respectively. In contrast, reaches were NO_3^- consumers, acting as sinks for NO_3-N during summer and autumn. NO_3^- load reductions were typically accompanied by striking declines in concentration, despite positive exchange potential (i.e., $+\Delta H_L$). Measured F_{eff} magnitudes for NO_3^- (-1.2 to -60.0 mg N m^{-2} d^{-1}) were similar to those reported in the literature associated with autotrophic N demand. Individual reaches occupied contrasting NPDs for NO_3-N and soluble reactive P by simultaneously serving as a sink for one and a source for the other. Hence, alternating reaches acted as enhancers or consumers, sequentially along the river, reflecting geologic and biological influences with implications for whole river behavior. The NPD approach combines routing influences of material exchange and local biological stream processes to provide a biogeochemical taxonomy for stream reaches with application to theory and practice.

Key words: nutrients, domains, uptake, load, source, sink, processing

Conceptual frameworks applied to lotic ecosystems have often embraced either a routing perspective, exemplified by the River Continuum Concept (Vannote et al. 1980) and the Nutrient Spiraling Concept (Newbold 1992), or models emphasizing local conditions, including patch dynamics (Townsend 1989, Rich et al. 2003), secondary succession (Fisher et al. 1982, Molles 1982), or island biogeography (Minshall et al. 1983). Yet, streams are influenced both by routing and local controls (Montgomery 1999, Valett et al. 2014), which combine to create heterogeneity in habitat (Thorp et al. 2006, Rosenfeld et al. 2007) and community composition (Grenouillet et al. 2004, Freixa et al. 2016). Emerging perspectives on streams have embraced the longitudinal development of ecosystem form

E-mail addresses: [4]maury.valett@umontana.edu; [5]mpeipoch@stroudcenter.org; [6]gpoole@montana.edu;
Correction: This article was reposted on May 6, 2022, to replace figure 6. Slope and CI values for panels C and D were changed.

Received 16 March 2021; Accepted 3 December 2021; Published online 6 May 2022. Associate Editor, Matthew Baker.

and function (Mctammany et al. 2003, Webster et al. 2009, Humphries et al. 2014), while recognizing the importance of finer scale modulation (Poole 2002, Burchsted et al. 2014), especially in terms of stream metabolism (Houser et al. 2005, Aristi et al. 2014, Bernhardt et al. 2018).

Similarly, perspectives on lotic biogeochemical structure have embraced multiple scales of organization. Large-scale patterns suggest upstream–downstream gradients reflecting solute enrichment and homogenization (Asano et al. 2009, Creed et al. 2015, Abbott et al. 2018). Some perspectives emphasize critical transitions in network size that are reflected in solute concentration, origin, and fate. Tiwari et al. (2017) reported 2 breaks in spatial and temporal variability in streamwater composition across 3 scaling domains that distinguished headwater streams from intermediate-sized and larger systems based on the progressive influence of groundwater. Abbott et al. (2018) argued that breakpoints in stream networks, where abrupt decline in chemical variance occurs, reflect spatial scales congruent with patch sizes serving as sources and sinks for a given solute. Also at the catchment level, spatial distribution and character of exchange between the stream and associated groundwater (Jencso et al. 2009, Mallard et al. 2014) may play a critical role in linking such patches to instream character along the course of a stream.

Lotic biogeochemical function also arises from processes at local and longitudinal scales. McGuire et al. (2014) suggested that spatial patterns of water chemistry in a 5th-order stream network depended on fine-scale processes and coarse-scale gradients attributed to instream and landscape controls. Mulholland et al. (2008) suggested that N-removal efficiency in streams declined with increasing stream size, attributing the reduction to a concomitant increase in N concentration. Tank et al. (2018) argued that patterns of N assimilation in small streams reflected spatial distribution of riparian cover, a feature of the aquatic–terrestrial interface that varies locally but progresses with increasing stream order (Gregory et al. 1991). At finer scales, instream nutrient processing can be influenced by debris dams (Munn and Meyer 1990), gravel bar interactions (Schade et al. 2001), and differential velocity distribution and associated biofilm behavior (Peipoch et al. 2016).

Controls on biogeochemical processes have been addressed at multiple spatial scales, but most studies of lotic biogeochemistry have assessed stream reaches hundreds to thousands of meters in length, a spatial scale conducive to field applications of spiraling (Newbold 1992), solute injection (Stream Solute Workshop 1990, Harvey and Wagner 2000), and mass-balance (Burns 1998, Lupon et al. 2020) approaches. However, despite the use of reaches as fundamental experimental units, little effort has been directed at developing a functional taxonomy of reach behavior.

Using a variety of metrics derived from data describing the change in stream discharge and solute concentration occurring within stream reaches, we propose nutrient processing domains (NPDs) as a categorization of reach character. Using data from a 20-y study of the Clark Fork River in western Montana, USA, we demonstrate how NPDs can be used to describe longitudinal patterns of biogeochemical processing along streams while identifying reaches with disproportional influence on whole-stream biogeochemistry.

NPDs

Drawing on ideas developed by Brinson (1993), who addressed wetland classification, and Montgomery (1999), who proposed geomorphic processing domains, we argue that the interaction of routing (e.g., flow accumulation and fluvial transport) and local (e.g., sessile benthic solute processing) controls forms distinct NPDs. We present the NPD approach as a functional taxonomy for stream reaches in the context of N and P, although the approach is applicable to any chemical constituent that is routed and processed within stream networks. An NPD is here defined as a distinct region within a multidimensional space defined by metrics describing the downstream change in stream discharge and solute concentration occurring within a stream reach. Thus, streams occupying the same NPD share similar biogeochemical character. The NPD concept is inherently budgetary, describing net alterations in nutrient load and concentration caused by the summed effects of water and nutrient delivery from the catchment and processes occurring within reach boundaries without distinguishing the ultimate origin of materials or their specific fates. Specifically, we classify reach character by considering the changes in discharge (Q, L^3/T), nutrient load (rate of downstream transport; L, M/T), and concentration (C, M/L^{-3}) that occur within the reach, with dimensions L = length, T = time, and M = mass. These changes can be expressed in relative (fractional) terms:

$$x_{\text{dwn:up}} = \frac{x_{\text{dwn}}}{x_{\text{up}}}, \qquad \text{(Eq. 1)}$$

where x can represent the downstream (dwn) and upstream (up) discharge ($Q_{\text{dwn:up}}$), load ($L_{\text{dwn:up}}$), or concentration ($C_{\text{dwn:up}}$), all dimensionless values.

Alternatively, we can characterize the difference between values at the downstream and upstream end of a designated reach:

$$\Delta x = x_{\text{dwn}} - x_{\text{up}}, \qquad \text{(Eq. 2)}$$

yielding ΔQ, ΔL, and ΔC. To facilitate inter-reach comparison, ΔQ and ΔL can be divided by reach area (A; L^2). Q normalized to reach area is hydraulic load (H_L, L/T; Kadlec and Wallace 2009), which reflects the ratio of total volumetric water delivery to the total streambed area. Because it normalizes stream Q to the area of the streambed, H_L allows for comparisons of the nature of water delivery among reaches of potentially very different wetted streambed area. Here, we normalize ΔQ to reach area as ΔH_L, the change in the areal rate of water delivery associated with transverse flow accumulation or loss within the reach (e.g., via tributaries, distributaries, diversions, withdrawals, evaporation, and groundwater exchange):

$$\Delta H_L = \frac{\Delta Q}{A}. \quad \text{(Eq. 3)}$$

Areal nutrient uptake (U, M L^{-2} T^{-1}) is commonly measured and reported in the nutrient spiraling literature (Newbold 1992, Webster and Valett 2007), typically calculated as the change in nutrient load assessed via tracers and normalized to reach streambed area. Similarly, ΔL normalized to reach area is the areal rate of net nutrient accumulation or loss from the water column along the reach, represented by the effective solute flux (F_{eff}, M L^{-2} T^{-1}). With this approach, F_{eff} represents the net rate of solute gain or loss/unit wetted area resulting from both advective and biotic processes within a given stream reach:

$$F_{\text{eff}} = \frac{\Delta L}{A}. \quad \text{(Eq. 4)}$$

Importantly, the mathematical sign of F_{eff} is opposite that typically reported for U in the literature. Consistent with mass-balance approaches, the sign of F_{eff} represents either removal ($-$) or addition ($+$) of dissolved nutrients.

Conceptually, F_{eff} can be parsed as the sum of advective and biotic changes in load:

$$F_{\text{eff}} = \frac{\Delta L_{\text{trans}} + \Delta L_{\text{bio}}}{A} = \frac{\Delta Q \times C_{\text{trans}}}{A} + \frac{\Delta L_{\text{bio}}}{A}, \quad \text{(Eq. 5)}$$

where ΔL_{trans} = change in nutrient load due to net transverse exchange including tributary inputs and interchange with groundwater, C_{trans} (M/L^3) is the mean solute concentration of transverse hydrologic inputs, and ΔL_{bio} is the net change in load due to biological processing. Accordingly, F_{eff} is related to ΔH_L and biological processing:

$$F_{\text{eff}} = \Delta H_L C_{\text{trans}} + F_{\text{bio}}, \quad \text{(Eq. 6)}$$

where F_{bio} is equivalent in magnitude to (but, as a component of mass balance, opposite in sign from) measures of U provided in the literature (Stream Solute Workshop 1990, Ensign and Doyle 2006).

These relationships yield measures of reach character. Change in Q, as absolute (ΔQ), relative ($Q_{\text{dwn:up}}$), or normalized (ΔH_L) metrics, represent the exchange potential—the possible influence of import and export. Absolute (ΔL) or normalized (F_{eff}) measures of load change reflect net material balance (NMB) for the system, where the mathematical sign characterizes the reach as either a source ($+$) or sink ($-$) for nutrients and the magnitude represents a measure of source/sink strength. Finally, $C_{\text{dwn:up}}$ represents the availability effect, reflecting processes that enrich, conserve, or deplete concentration, with implications for biota within the reach's stream channel. As such, character is a collective property that arises from the interaction of routing and local processing, which alter the chemical environment and can be used to assign a reach to an NPD of a given biogeochemical profile.

NPD identities

Complete assessment of nutrient delivery and fate within a given reach entails knowing the concentrations of accumulating stream waters and discerning the influences of different instream processes (e.g., assimilation, mineralization, dissimilatory reduction, oxidation, and fixation) along with the implications of material exchange. Such characterization typically requires empirical measures of biological and hydrologic behavior via tracer and spiraling approaches (e.g., Peterson et al. 2001, Mulholland et al. 2008, Covino et al. 2010). Although our mass-balance approach cannot provide such distinction, diagnostic assessment of NMB, exchange potential, and the availability effect can be accomplished via quantification of F_{eff}, ΔH_L, and $C_{\text{dwn:up}}$, respectively. Further, we argue that distinct combinations of these attributes characterize extant NPDs that arise as a result of the physical, chemical, and biological character of individual river reaches. Thus, NPDs can be visualized through diagnostic plots relating F_{eff} (material balance) to $C_{\text{dwn:up}}$ (change in availability) with greater ΔH_L reflected by increasing symbol size. With this approach, we propose 5 commonly occurring NPDs (Table 1) characteristic of streams and rivers that entail most reach biogeochemical behavior (Fig. 1).

Reaches with positive NMB ($+F_{\text{eff}}$) are source reaches while those with negative NMB ($-F_{\text{eff}}$) are sink reaches. In this way, the terms source and sink generally describe reach types because they represent the net effects of both transport and processing but do not reflect the ultimate origin or fates of any solute of interest. The strongest sources are commonly associated with substantial ΔH_L (vertical arrow; Fig. 1). Sources can act as enhancers ($C_{\text{dwn:up}} > 1$) when transverse water inputs are of greater concentration than reach water or via endogenous benthic solute production. When sources accumulate both flow and load in proportion, the reaches display neither depletion nor enrichment (i.e., $C_{\text{dwn:up}} \approx 1$) and can be thought of as compilers. Sources may display depletion (i.e., $C_{\text{dwn:up}} < 1$) but must operate through dilution (i.e., diluters; Fig. 1). Most commonly, this would occur when tributaries, groundwater, or other flow accumulations are lower in concentration than reach water (e.g., during snowmelt runoff; Williams and Melack 1991).

Reaches that serve as sinks ($F_{\text{eff}} < 0$) have –, neutral, or slightly $+\Delta H_L$. Moreover, sink reaches displaying depletion of nutrient availability ($C_{\text{dwn:up}} < 1$) can be considered consumers. Streams with $+\Delta H_L$ will be depleting sinks (i.e., consumers) if the magnitude of F_{bio} exceeds the advective load (i.e., $-F_{\text{bio}} > \Delta H_L C_{\text{trans}}$; Eq. 6). From this perspective, F_{eff} in depleting sinks with non-negative ΔH_L can generally be viewed as a conservative estimate of U. Streams with

Table 1. General definitions and common drivers of 5 distinct nutrient processing domains (NPDs). Each NPD is defined as an area of the multidimensional functional space created by exchange potential, material balance, and availability.

NPD	Domain definition	Common drivers
Enhancer	A source area of solute enrichment via endogenous or exogenous origins that increase solute loads and concentrations	Natural geogenic and organic sources, agricultural and urban pollution
Diluter	A source area of solute depletion resulting in decreased concentration but increased load through water and solute gain along the river channel	Snowmelt, heavy rains
Compiler	A source area characterized by equilibrium between enrichment and depletion processes where solute concentrations remain unchanged and load increases commensurate with hydrologic accumulation	Flow accumulation from sources of comparable concentration, coincidental balance between uptake and release mechanisms
Consumer	A sink area of load decrease typically associated with solute depletion via biological removal	High rates of biological growth, assimilatory demand and dissimilatory removal
Conduit	An area of material steady state where processes of import and production are equal to the combined effects of export and removal resulting in conservation of concentration and load (i.e., pipe behavior)	Constrained reaches in hydrologic balance, low biological activity, or mature biotic communities in metabolic steady state

$-\Delta H_L$ are also generally depleting sinks because they are biotically active and export solutes via hydrologic exchange flows.

When a reach is in material balance ($F_{\mathrm{eff}} \approx 0$), the reach functions as a conduit and typically has either little ΔH_L and little F_{bio} or has values of F_{bio} and $\Delta H_L C_{\mathrm{trans}}$ that are similar in magnitude but opposite in sign. The latter case would be associated with a modest $+\Delta H_L$ and, therefore, would also exhibit modest depletion of availability. As with the exceptions to the generalities for depleting sinks, a conduit with $+\Delta H_L$ is possible without F_{bio} but requires a mechanism for removing some flow from the stream while gaining more flow than is removed, as may be encountered in karst landscapes (Gibert et al. 1994).

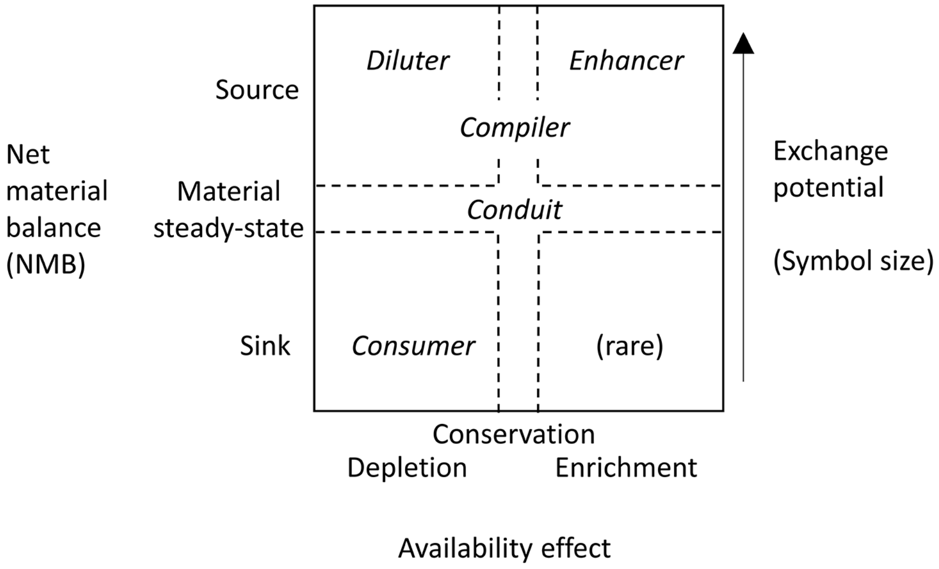

Figure 1. Nutrient processing domains (NPDs, italicized) reflecting reach behavior in functional space defined by applicable measures of net material balance (NMB), the availability effect, and exchange potential. Exogenous influence associated with increasing exchange potential is represented by larger symbols. The arrow associated with exchange potential represents anticipated association of increasing exchange potential with NPDs heavily influenced by flow accumulation. Graphical representation thus displays all 3 measures of biogeochemical character that result in occupation of a specific NPD. Dashed lines bound realms of functional space not different from the null values for availability (conserved downstream-to-upstream concentration, $C_{\mathrm{dwn:up}} = 1$) and NMB (material steady state effective solute flux, $F_{\mathrm{eff}} = 0$).

Here we employ the NPD approach in a case study of the Upper Clark Fork River (UCFR), Montana, USA, where water quality is challenged by both historical mining activities and anthropogenic N inputs (Moore and Langner 2012, Suplee et al. 2012). Based on historical records of river flow and nutrient concentrations derived from long-term (20 y) monitoring, we employ NPD assessment both as a paradigm for addressing biogeochemical function and as an approach to understanding applied issues associated with water quality and resource management in running-water systems.

METHODS

To illustrate the application and benefits of an NPD approach, we first coupled measures of river flow with nutrient concentrations to quantify material loads and their alteration along designated river reaches. We then derived measures of NMB, ΔH_L, and availability that we assessed as distinct metrics for each reach seasonally and across nutrient forms. Using these metrics, we placed reaches into appropriate NPDs across time and space to interpret biogeochemical character.

Study site

The UCFR is a 4th-order, open-canopied river that drains the western flank of the continental divide (lat 46.187150, long −112.769960), Montana, USA. The river has a long history of mining contamination. Following a massive flood in 1908, mine tailings containing heavy metals were distributed and deposited throughout the UCFR's channel and floodplain (Moore et al. 1989, Nimick and Moore 1993). The river is presently part of the largest United States Environmental Protection Agency (USEPA) Superfund site, with hundreds of millions of US dollars dedicated to remediating and restoring the river's floodplain and tributaries over the next 20 y (Montana Department of Justice 2012).

Beyond heavy metal contamination, USEPA assessment also identified nutrient loading as a critical factor creating aquatic life problems in the UCFR. Nutrient enrichment in the UCFR, including elevated concentrations of NO_3^- and periodic algal blooms promoted by nutrient-rich conditions in sunlit river water, motivated the establishment of some of the 1st-ever river water-quality standards in the US, including an algal biomass criterion of 100 mg/m^2 as chlorophyll *a* (Chl *a*; Dodds et al. 1997, Suplee et al. 2007). Algal standing crops in the UCFR are dominated by *Cladophora* spp. and can frequently reach nuisance levels as great as 600 mg Chl *a*/m^2 (Watson 1989, Suplee et al. 2012). Blooms in the UCFR can lead to low dissolved oxygen levels in river water, impair river aesthetics, and ultimately influence irrigation and recreational activities (Ingman 1992).

Long-term dataset

Long-term patterns in physicochemical characteristics of the UCFR were evaluated from a historic dataset derived and compiled from original data acquired by the Tri-State Water Quality Council (2009) (Suplee et al. 2012). We restricted our geographic extent of analysis to the upper ½ of the UCFR's 200-km length (Fig. 2), incorporating 4 monitoring sites that delineate 3 study reaches (I–III), spatially contiguous along the first 85 km downstream from the river's origin. Over this distance, the drainage basin grows from 1699 to 4595 km^2, and average annual runoff increases from 4.3 to 14.5 m^3/s.

The dataset (Table S1) includes all complete annual records of water quality and discharge measurements collected biweekly during each month between 1986 and 2005. All samples collected during the first 2 wk, or last 2 wk, of any given month were considered part of the same sampling event and were averaged to a single measure. With this approach, complete annual records with biweekly samples were available for 11 y including 1986 to 1992, 1999 to 2001, and 2005. For seasonal assessment, data were aggregated for summer (July–September), autumn

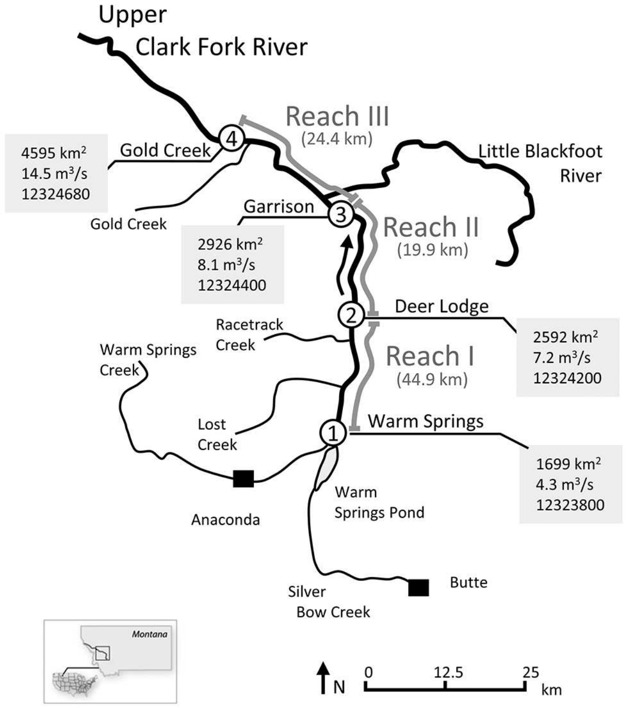

Figure 2. Map of the study area on the Upper Clark Fork River (UCFR), Montana, USA, showing 4 long-term monitoring locations (circled numbers) and intervening study reaches (I–III), along with their significant tributaries. UCFR catchment area, average annual discharge (1984–2013), and United States Geological Survey gauge numbers associated with each of the monitoring locations are provided in the gray boxes. Historical mining operations in Butte and Anaconda (black squares) located on Warm Springs and Silver Bow creeks led to the construction of Warm Spring Pond at the origin of the UCFR for the purpose of retaining metal contaminated sediments. Arrow between sites 2 and 3 indicates direction of flow.

(October–November), winter (December–February), and spring (March–June) to reflect seasonality representative of the temperate climate of the Rocky Mountain region of Montana.

We obtained river discharge data from United States Geological Survey (USGS) gauging stations at the 4 sample sites (Fig. 2). Discharge for any sampling was averaged over the 2-wk period during which water quality was measured. Occasional gaps in discharge were filled via correlational relationships with USGS data from the nearest gauging station.

We derived reach lengths (Fig. 2) from 2018 Google Earth images (earth.google.com) and assumed them to be constant over the duration of the analysis. Reach width was represented by the mean value of the wetted channel width as determined from USGS gauge data applicable to the head and the base of each reach. At each location, wetted width was related to stream flow via best-fit regression models ($n = 111$–431). Widths were derived for 2-wk periods and multiplied by reach length to determine wetted area for each mass-balance assessment.

Along with water temperature (°C), water-quality measures addressed here include inorganic N as NH_4-N and NO_3-N, along with soluble reactive P (SRP) as a representative of bioavailable (i.e., inorganic) P, and measures of total N (TN) and total P (TP) derived from unfiltered samples. Atomic N:P ratios were generated from molar ratios of inorganic N (NH_4-N + NO_3-N) and bioavailable P (i.e., SRP). Concentrations of NH_4-N were generally low compared to NO_3-N, and analyses of transport and uptake for inorganic N forms were restricted to NO_3-N. Field and laboratory methods employed during historical monitoring (Table S1) are detailed in Suplee et al. (2012).

Data analysis

To assess reach-scale changes in hydrologic and biogeochemical metrics within and among sites and reaches, we relied on biweekly measures and seasonal aggregations to derive measures of central tendency and variation of ln-transformed values. We back-transformed and corrected measures before presenting means and 95% CIs. All calculations were performed using the Statistical Analysis System (version 9.4; SAS Institute, Cary, North Carolina).

Because of spatial and temporal interdependence among data, we did not employ inferential statistics to address differences in metrics among reaches or seasons (Hurlbert 1984). Instead, we assessed 95% CIs to distinguish substantial differences (i.e., when CIs for means did not overlap) from those that were less evident. We used this approach to compare measures of stream flow (Q_{dwn}, ΔQ, $Q_{dwn:up}$, ΔH_L), nutrient concentrations (NH_4-N, NO_3-N, TN, TP) and atomic N:P ratios among seasons and reaches. The same approach was used to address spatial and temporal differences in F_{eff} and $C_{dwn:up}$. We also used 95% CIs to address whether mean values for changes in nutrient concentrations and loads within a given reach and season differed from null values, reflecting a lack of change. Specifically, we identified nutrient F_{eff} and $C_{dwn:up}$ changes as substantially different from 0 and 1, respectively, when 95% CIs for ln-transformed data did not include the appropriate adjusted and ln-transformed null values.

For each reach, we used linear models to compare seasonal mean values for F_{eff} derived for each year of assessment ($n = 11$) with seasonal mean values for flow accumulation (ΔH_L). Because of temporal interdependence between metrics, we report the regression coefficients (i.e., slopes [b]) and associated 95% CIs along with the standardized slopes (i.e., correlation coefficients [r]), but without inferential assessment of the coefficients' variance, which is biased because of auto-correlation.

RESULTS

Hydrology

Stream flow showed distinctive seasonal patterns across reaches but differed in magnitude among reaches. Consistent with snowmelt-dominated catchments, maximal stream flow occurred during spring across all reaches (Fig. 3A), when mean Q ranged from 6.32 to 13.94 m^3/s (Table 2). Stream flow was lower in summer than during other seasons. All mean values addressing differences in Q into and out of study reaches ($Q_{dwn:up}$, ΔQ, ΔH_L) illustrated substantial net flow accumulation across all reaches and seasons (Table 2). Flow in reach I increased by 0.71 to 3.18 m^3/s, a factor of 1.4 to 2.3, corresponding to increases in H_L from 0.08 to 0.33 m/d. Greatest flow accumulation in reach I occurred in winter, as indicated by higher values for all measures of change in Q compared with other seasons (Table 2). In reach II, the magnitude of flow increase was smaller ($\Delta Q = 0.37$–0.55 m^3/s) and generally did not differ among seasons, resulting in changes of <10% from autumn through spring and 14% in summer. Maximal ΔH_L in reach II was 0.09 m/d during winter, a value only slightly greater than the minimum observed in reach I. Greater flow accumulation occurred in reach III ($\Delta Q = 2.54$–7.50 m^3/s) where ΔH_L ranged from 0.29 to 0.80 m/d with greatest ΔH_L during spring (Table 2). Across all study reaches, negative values for ΔQ represented 11, 13, and 4% of all observations in reaches I, II, and III, respectively, and were rarely observed (15 of 45 occurrences) during summer and autumn baseflow conditions.

Nutrient concentrations

Based on grand means derived from all monitoring dates, nutrient concentrations differed among sites, with different patterns among nutrients. NH_4-N concentrations were greatest at site 1 (0.024 mg/L), and concentrations at sites further downstream were lower and similar, ranging from 0.009 to 0.013 mg/L (Table 3). Mean NO_3-N (0.148 mg/L) and TN (0.549 mg/L) concentrations were maximal at site 2 (Table 2). In contrast, concentrations of SRP

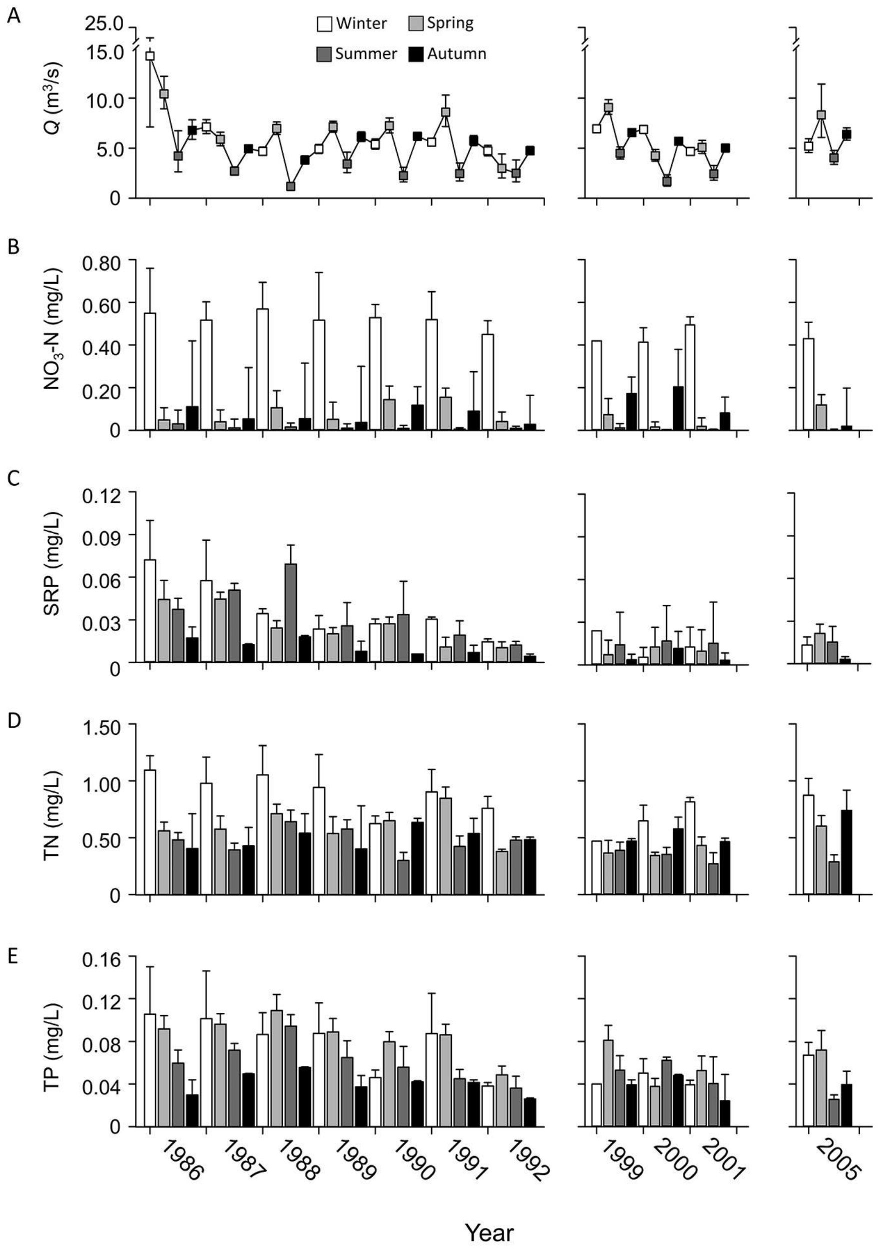

Figure 3. Seasonal changes in flow and water chemistry over the monitoring period at the Upper Clark Fork River, Montana, USA: river discharge (Q; A), NO_3-N (B), soluble reactive P (SRP; C), total N (TN; D), and total P (TP; E). Data are back-transformed seasonal means within years for river flow (±SE) and chemical constituents (+SE) at Site 3. Similar plots for sites 1, 2, and 4 are available in Figs S1–S3.

(0.007 mg/L) and TP (0.037 mg/L) were lower at site 2 than at any other location (Table 3). Accordingly, atomic N:P ratios at site 2 were maximal (50.9) and greater than at all other sites where averages ranged from 7.4 to 10.2 (Table 3).

Solute concentrations in the UCFR also exhibited seasonal patterns, with maximum concentrations in winter and minima during either summer or autumn (Figs 3B–E, S1–S3). Maximum NO_3-N concentrations (data not shown) averaged 0.310 and 0.505 mg/L at sites 1 and 2, respectively, and were ~4 to 5× their corresponding minimum values (0.048 and 0.094 mg/L). In comparison, maxima at sites 3 (0.491 mg/L) and 4 (0.372 mg/L) were 50× greater than minima (0.010 and 0.007 mg NO_3-N/L for sites 3 and 4, respectively). SRP concentration was greatest during winter (0.016–0.029 mg/L) and lowest in autumn (0.004–0.010 mg/L), and relative variation over annual time frames was particularly constrained for all sites (3.3–3.7×; Figs 3C, S1–S3). Annual patterns of TN (Figs 3D, S1–S3) were like those observed for NO_3-N, but winter maxima (0.624–0.832 mg/L) were only 1.8 to 2.4× the minimum

Table 2. Seasonal assessment of reach hydrologic behavior, including river discharge at the downstream site (Q_{dwn}), change in discharge (ΔQ) over the length of the reach, associated change in hydraulic load (ΔH_{L}), and ratio of discharge comparing downstream to upstream sites (Q_{dwn}:Q_{up}) for each of the 3 river reaches in the Upper Clark Fork River, Montana, USA. Values are mean, lower 95% CL (LCL), upper 95% CL (UCL), and number of observations (*n*) based on biweekly sampling during each season over the 11 y analyzed. All analyses were done on ln-transformed data. Table values for means and CLs have been back-transformed.

		Q_{dwn} (m^3/s)				ΔQ (m^3/s)				ΔH_{L} (m/d)				Q_{dwn}:Q_{up}			
Reach	Season	Mean	LCL	UCL	*n*	Mean	LCL	UCL	*n*	Mean	LCL	UCL	*n*	Mean	LCL	UCL	*n*
I	Winter	5.43	4.62	6.37	32	3.18	2.36	4.09	32	0.33	0.21	0.40	32	2.35	2.11	2.61	32
	Spring	6.32	5.57	7.18	69	1.66	1.12	0.20	69	0.19	0.11	0.20	69	1.48	1.36	1.60	69
	Summer	2.32	1.85	2.91	38	0.71	0.36	1.08	38	0.08	0.03	0.09	38	1.43	1.23	1.65	38
	Autumn	5.11	4.66	5.59	22	2.62	2.26	3.00	22	0.27	0.19	0.26	22	2.18	1.91	2.48	22
II	Winter	5.91	4.98	7.02	31	0.55	0.15	0.98	31	0.09	0.02	0.16	31	1.08	1.05	1.11	31
	Spring	6.70	5.90	7.61	69	0.37	0.19	0.56	69	0.06	0.03	0.09	69	1.06	1.03	1.09	69
	Summer	2.78	2.30	3.38	38	0.40	0.32	0.48	38	0.07	0.06	0.08	38	1.20	1.14	1.26	38
	Autumn	5.57	5.12	6.05	22	0.44	0.26	0.61	22	0.07	0.0	0.10	22	1.09	1.06	1.13	22
III	Winter	8.91	7.39	10.74	31	3.18	2.05	4.48	31	0.35	0.18	0.49	31	1.51	1.41	1.61	31
	Spring	13.94	12.24	15.87	68	7.50	6.58	8.74	68	0.80	0.61	0.85	68	2.11	1.97	2.25	68
	Summer	5.12	4.32	6.07	34	2.54	2.08	3.02	34	0.29	0.21	0.30	34	1.96	1.77	2.15	34
	Autumn	8.57	7.87	9.33	22	3.03	2.75	3.35	22	0.31	0.25	0.31	22	1.54	1.50	1.58	22

values observed in summer (0.298–0.44 mg/L). Like SRP, temporal change in TP was constrained. Maximum concentrations in spring (0.045–0.068 mg/L) were only 1.3 to 1.8× greater than minima (0.024–0.039 mg/L) observed in summer (Figs 3E, S1–S3).

F_{eff}, availability, and ΔH_L

Nutrient loading (kg/d) to the head of each reach differed with season and reach (Tables S2, S3). Maximum NO_3-N loads (55.5–232.2 kg/d) occurred in winter and were 14 to 117× the minimum loading rates observed during summer (2.0–15.9 kg/d). Winter NO_3-N loads were greater than during all other seasons and occurred when concentrations were greatest (Figs 3, S1–S3) and flows were comparable to those in spring (Table 2). In contrast, maximal loads for SRP (3.9–11.0 kg/d; Table S2) and TP (22.0–45.0 kg/d; Table S3) generally occurred in spring and were substantially greater than the minimum loads (SRP = 1.1–3.4 kg/d, TP = 4.7–11.8 kg/d) observed during summer and autumn. Winter and spring loading rates for TN (115.1–387.5 kg/d) were similar and elevated compared to other seasons, whereas summer loads (51.6–93.3 kg/d) were consistently lowest among seasons. The relative increases in loading rates for SRP, TP, and TN observed during winter and spring (3.3–6.4×) were lower than those observed for NO_3-N.

Temporal patterns of load changes along the length of study reaches (Tables S2, S3) generated F_{eff} that differed among reaches and progressed with season (Fig. 4A–D). In reach I, F_{eff} for NO_3^- ($F_{\mathrm{eff\text{-}NO3}}$) was positive and substantially >0 during all seasons (Fig. 4A). Fluxes were maximal in winter (194.7 mg N m^{-2} d^{-1}) and declined more

Table 3. Concentrations of NH_4-N, NO_3-N, soluble reactive P (SRP), atomic N-to-P ratio (atomic N:P), total N (TN), and total P (TP) for the 4 monitoring sites at the Upper Clark Fork River, Montana, USA. Values are grand means ($\bar{x}$), lower 95% CL (LCL), upper 95% CL (UCL), and number of observations (*n*) based on biweekly sampling over the 11 y analyzed. All analyses were done on ln-transformation data. Table values for means and CLs have been back-transformed.

	Site1				Site 2				Site 3				Site 4			
Analyte	$\bar{x}$	LCL	UCL	*n*	$\bar{x}$	LCL	UCL	*n*	$\bar{x}$	LCL	UCL	*n*	$\bar{x}$	LCL	UCL	*n*
NH_4-N	0.024	0.021	0.028	160	0.009	0.008	0.011	160	0.013	0.011	0.015	159	0.010	0.008	0.011	154
NO_3-N	0.057	0.048	0.069	157	0.148	0.125	0.174	159	0.058	0.043	0.078	158	0.034	0.025	0.045	154
SRP	0.013	0.011	0.016	160	0.007	0.006	0.008	160	0.013	0.015	0.021	159	0.017	0.015	0.019	153
Atomic N:P	10.2	8.2	12.7	140	50.9	42.0	61.6	159	10.7	8.1	14.1	158	7.4	5.7	9.5	153
TN	0.441	0.409	0.476	159	0.549	0.513	0.587	159	0.538	0.500	0.580	158	0.413	0.379	0.450	152
TP	0.049	0.045	0.054	160	0.037	0.034	0.031	160	0.060	0.055	0.065	160	0.050	0.046	0.054	154

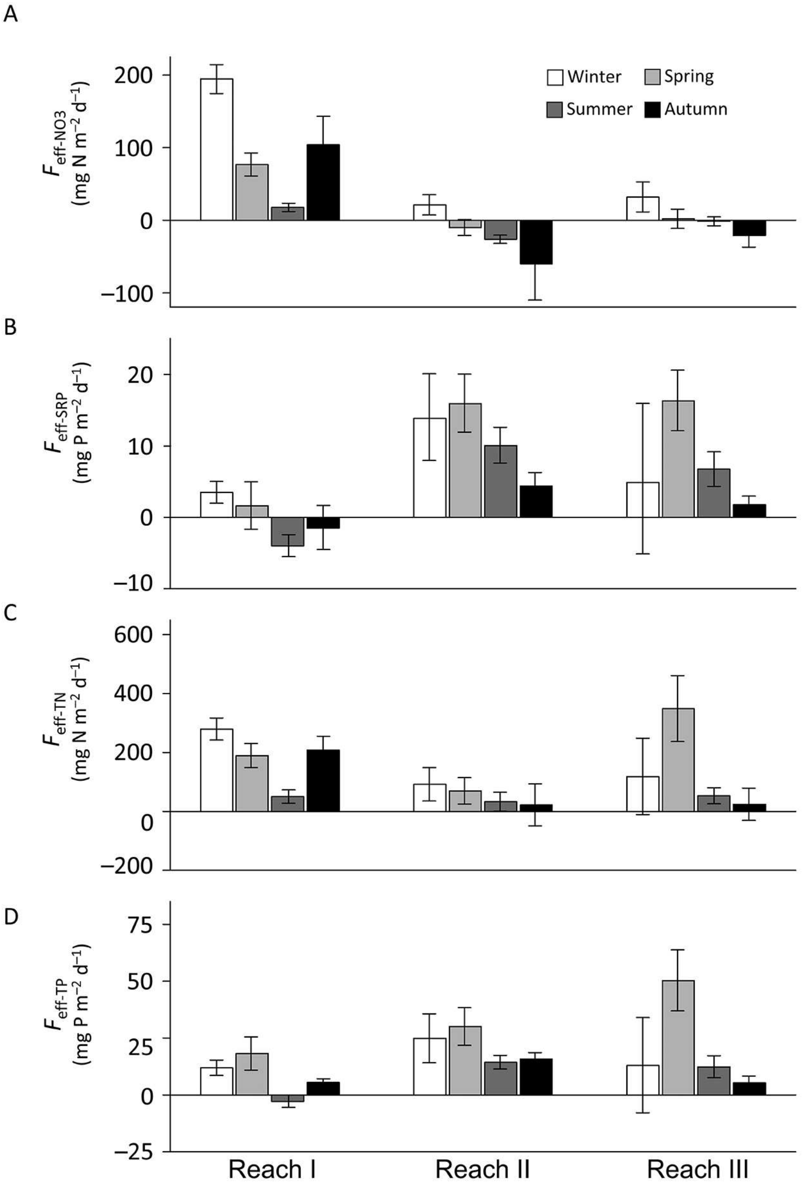

Figure 4. Effective solute flux (F_{eff}, mg m^{-2} d^{-1}) for NO$_3$-N (A), soluble reactive P (SRP; B), total N (TN; C), and total P (TP; D) in the Upper Clark Fork River, Montana, USA. Within a panel and reach, data are back-transformed means ±95% CI by season for reaches I (n = 22–68), II (n = 22–68), and III (n = 22–67). Horizontal line in each panel designates $F_{\text{eff}} = 0$ and distinguishes positive from negative values associated with net load increases or decreases, respectively.

than an order of magnitude by summer (17.6 mg N m^{-2} d^{-1}) before increasing again during autumn. Observed concentrations for NO$_3^-$ in water leaving reach I were consistently greater than those for water entering the reach with $C_{\text{dwn:up}}$ for NO$_3^-$ ($C_{\text{dwn:up-NO3}}$) indicating substantial increases in concentration across all seasons (Fig. 5A). Concentrations increased by as little as 1.7× in winter to 3.7× in summer (Fig. 5A). In contrast, reach II was a sink for NO$_3$-N during spring, summer, and autumn and was a source only during winter (Fig. 4B). From spring through autumn, $F_{\text{eff-NO3}}$ became increasingly negative (−10.1 to −60.0 mg N m^{-2} d^{-1}), and values were substantially <0 during summer and autumn. During winter, load increases within reach II occurred without substantial change in concentration ($C_{\text{dwn:up-NO3}}$ not different from 1; Fig 5A). In contrast, declines in NO$_3$-N load along reach II observed from spring through autumn (Table S2) were accompanied by $C_{\text{dwn:up-NO3}}$ values well below 1 (Fig. 5A), reflecting decreases in NO$_3$-N concentrations such that downstream concentrations in summer were an order of magnitude lower than those recorded upstream. Transition from source to sink for NO$_3$-N also occurred in reach III (Fig. 4A) as $F_{\text{eff-NO3}}$ changed progressively from

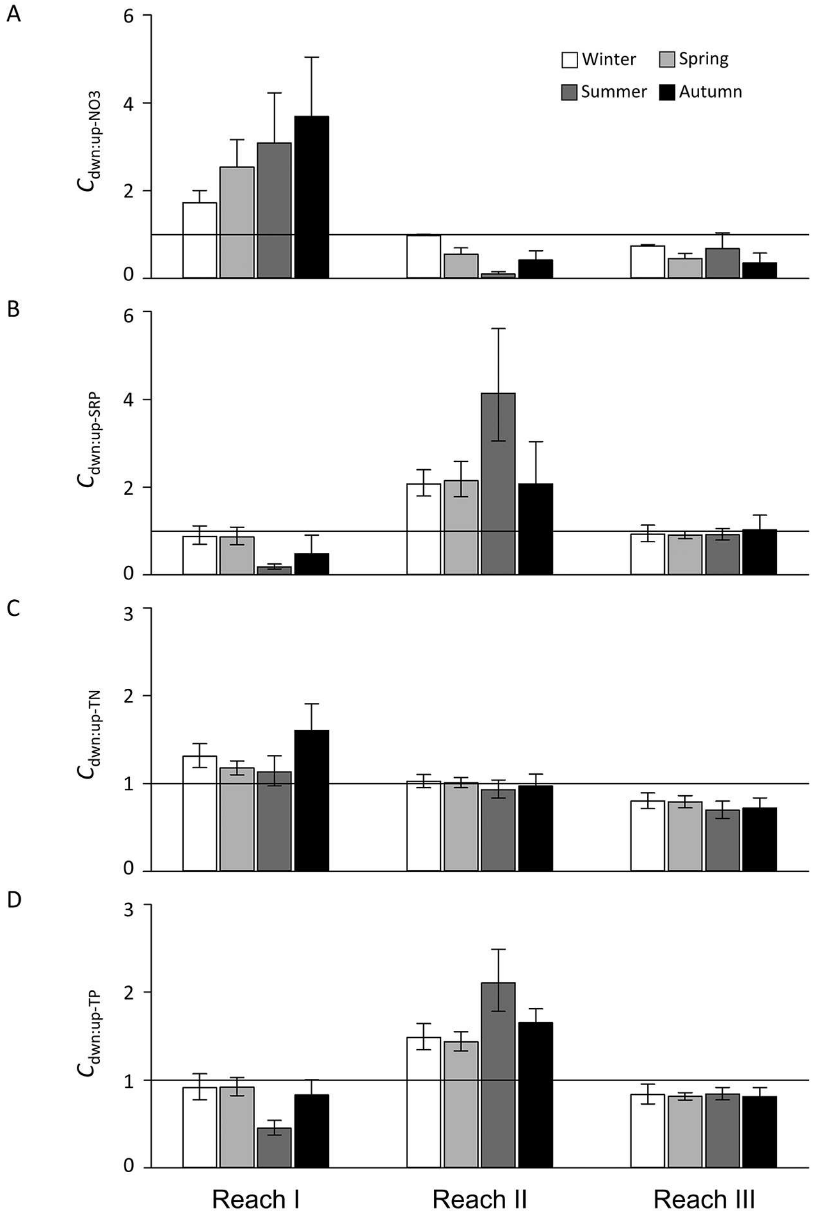

Figure 5. Ratio of downstream-to-upstream concentration ($C_{\text{dwn:up}}$) for NO_3-N (A), soluble reactive P (SRP; B), total N (TN; C), and total P (TP; D) at the Upper Clark Fork River, Montana, USA. Within a panel and reach, data are back-transformed means ±95% CI by season for reaches I ($n = 22$–68), II ($n = 22$–68), and III ($n = 22$–67). Horizontal line in each panel designates $C_{\text{dwn:up}} = 1$ indicating no change in concentration from upstream to downstream sampling sites.

substantially positive in winter (26.9 mg N m^{-2} d^{-1}) to substantially negative (-17.5 mg N m^{-2} d^{-1}) in autumn. All stages of progression from a winter NO_3-N source to an autumnal sink were accompanied by declines in concentration (Fig. 5A).

Patterns of F_{eff} for SRP ($F_{\text{eff-SRP}}$) were opposite those observed for $F_{\text{eff-NO3}}$ (Fig. 4B). Reach I was a consistent source for NO_3-N, but substantial accumulations of SRP occurred in reach I only during winter (3.2 mg P m^{-2} d^{-1}; Fig. 4B), while the positive mean value for $F_{\text{eff-SRP}}$ in spring was not substantially different from 0. $F_{\text{eff-SRP}}$ became negative (-3.6 mg P m^{-2} d^{-1}) during summer and remained negative (-1.3 mg P m^{-2} d^{-1}), but not substantially different from 0, during autumn. During the seasonal progression from source to sink, SRP concentrations ($C_{\text{dwn:up-SRP}}$) remained unchanged during winter and spring but declined substantially during summer and autumn (Fig. 5B). In reach II, substantial and strongly positive values for $F_{\text{eff-SRP}}$ were observed across all seasons (5.1–16.0 mg P m^{-2} d^{-1}; Fig. 4B). Positive $F_{\text{eff-SRP}}$ values were accompanied by strong increases in $C_{\text{dwn:up-SRP}}$ (substantially >1; Fig. 5B), reflecting

2× increases in $C_{\text{dwn:up-SRP}}$ in spring, autumn, and winter, and a 4× increase in summer. Thus, reach II functioned as an enriched and robust source of SRP, whereas it served primarily as a NO_3-N sink (Fig. 4A). Reach III also functioned as a strong SRP source with consistently positive $F_{\text{eff-SRP}}$ values (2.0–19.0 mg P m^{-2} d^{-1}; Fig. 4B) of magnitudes similar to those observed in reach II. At the same time, the mean value for $C_{\text{dwn:up-SRP}}$ in reach III was not substantially different than 1 during any season (Fig. 5B), indicating that net load accumulation (Fig. 4B) occurred without changes in $C_{\text{dwn:up-SRP}}$.

Solute F_{eff} for TN ($F_{\text{eff-TN}}$) and TP ($F_{\text{eff-TP}}$) were of greater magnitude, but not as seasonally dynamic, as those observed for $F_{\text{eff-NO3}}$ or $F_{\text{eff-SRP}}$, respectively (Fig. 4A–D). In general, all reaches acted as TN and TP sources with greatest $F_{\text{eff-TN}}$ (91.8–348.5 mg N m^{-2} d^{-1}) and $F_{\text{eff-TP}}$ (18.2–50.2 mg P m^{-2} d^{-1}) during winter or spring and lowest values in summer and autumn. In reach II, however, $F_{\text{eff-TN}}$ (32.8–91.8 mg N m^{-2} d^{-1}) was generally lower than in other reaches and not different from 0 during summer and autumn (Fig. 4C). Mean values for $C_{\text{dwn:up-TN}}$ did not differ substantially from 1 across seasons (Fig. 5C). Together, these data indicate little change in TN load or concentration over the course of reach II during any season. In reach III, positive seasonal means for $F_{\text{eff-TN}}$ were substantially >0 during spring and summer (Fig. 4C), but TN concentrations declined substantially from upstream to downstream ($C_{\text{dwn:up-TN}} < 1$; Fig. 5C) during all seasons.

All $F_{\text{eff-TP}}$ measures were positive across the 3 reaches except during summer in reach I, when a negative mean value (−2.5 mg P m^{-2} d^{-1}; Fig. 4D) indicated substantial load decline, closely resembling SRP behavior in the same reach (Fig. 4B). Observed downstream concentrations for TP were substantially lower than upstream in reach I during summer and during all seasons in reach III but 1.4 to 2.1× greater than upstream in reach II (Fig. 5D). As such, TP concentration tended to remain unchanged along reach I, but declined in summer as the reach changed from source to sink, always increased in reach II, which served as a robust source, and always declined along reach III despite the reach acting as a substantial TP source during all seasons but winter (Figs 4D, 5D).

Reach characterization

F_{eff} and ΔH_L should be positively related (Eq. 6) because exchanging waters carry some amount of solute, with implications for material loads. A scatterplot of F_{eff} and ΔH_L illustrates variation in the nature of this relationship among the 4 solutes and 3 reaches (Fig. 6A–D). Based on seasonal means from each of the 11 y of monitoring, reaches can be placed into 4 quadrants (designated by dashed lines in Fig. 6A–D and defined in panel B) defined by the direction of each flux. Across solutes, reaches, and seasons, ΔH_L ranged from −0.04 to 1.2 m/d, with only 9 of 132 observations <0. Most observations were in the 1st quadrant, representing reaches with flow accumulation (i.e., $+\Delta H_L$) that simultaneously behaved as solute sources (i.e., $+F_{\text{eff}}$). The percentage of observations associated with increasing hydrologic and material loads, however, differed among solutes. For TP and TN, respectively, 83.0 and 80.7% of all observations were found in quadrant I. The percentages for SRP and NO_3-N were lower, with only 76.3 and 62.2% of observations, respectively, found in quadrant I. Because so few measures of ΔH_L indicated net loss of water from the reach (Fig. 6A–D), no more than 5.9% of observations represented losing reaches that either gained (quadrant II) or lost (quadrant III) mass of any given solute. The percentage of observations found in quadrant IV, where ΔH_L was positive but reaches acted as net sinks (i.e., $F_{\text{eff}} < 0$), differed among solutes of contrasting bioavailability. For TP and TN, 9.6 and 12.6% of observations, respectively, were found in quadrant IV. Percentages for SRP and NO_3-N were much higher (17.9 and 31.3%, respectively), indicating greater propensity for gaining reaches to act as sinks for SRP and NO_3-N relative to TP and TN.

The propensity for the magnitude of F_{eff} to be closely associated with ΔH_L depended on solute identity. For mean values among all reaches and seasons, the relationships between F_{eff} and ΔH_L for NO_3-N ($r = 0.21$; Fig. 6A) and SRP ($r = 0.37$; Fig. 6B) were weaker than those observed for TN ($r = 0.70$; Fig. 6C) and TP ($r = 0.58$; Fig. 6D). For NO_3-N, these variables were closely related only in reach I ($r = 0.69$; Fig. S4A) and were poorly related in all other reaches ($r = 0.05$ and 0.06; Fig. S4B, C). For SRP, they were positively and strongly related in both reaches I and III ($r = 0.57$ and 0.66, respectively; Fig. S4D, F), but not in reach II ($r = 0.19$; Fig. S4E). For TN and TP, not only were F_{eff} and ΔH_L related across all observations, but exchange and solute flux were closely related within reaches independently for both solutes (Fig. S5A–F). Correlation coefficients reflecting the degree of congruence between F_{eff} and ΔH_L were generally higher for TN than for TP (Fig. S5A–F) and were lowest in reach II regardless of the solute (Figs S4B, E, S5B, E).

NPD occupation: NMB, availability effect, and ΔH_L

Using mean values for F_{eff}, $C_{\text{dwn:up}}$, and ΔH_L derived for each reach and season across the 11 y of assessment as representative of NMB, the availability effect, and exchange potential, we employed diagnostic plots of solute dynamics to portray the functional distribution and seasonal progression of UCFR reaches among the NPDs (Fig. 7A–D). For NO_3-N, reach I consistently and exclusively behaved as an enhancer, but it displayed substantial interannual variation in the degree to which it functioned as a source, the extent of associated enrichment, and the magnitude of the exchange effect (Fig. 7A, circles). In contrast, reaches II and III seasonally transitioned from source to sink over the annual cycle. During winter, both reaches behaved as compilers, with load accumulations generally accompanied by conserved or depleted availability

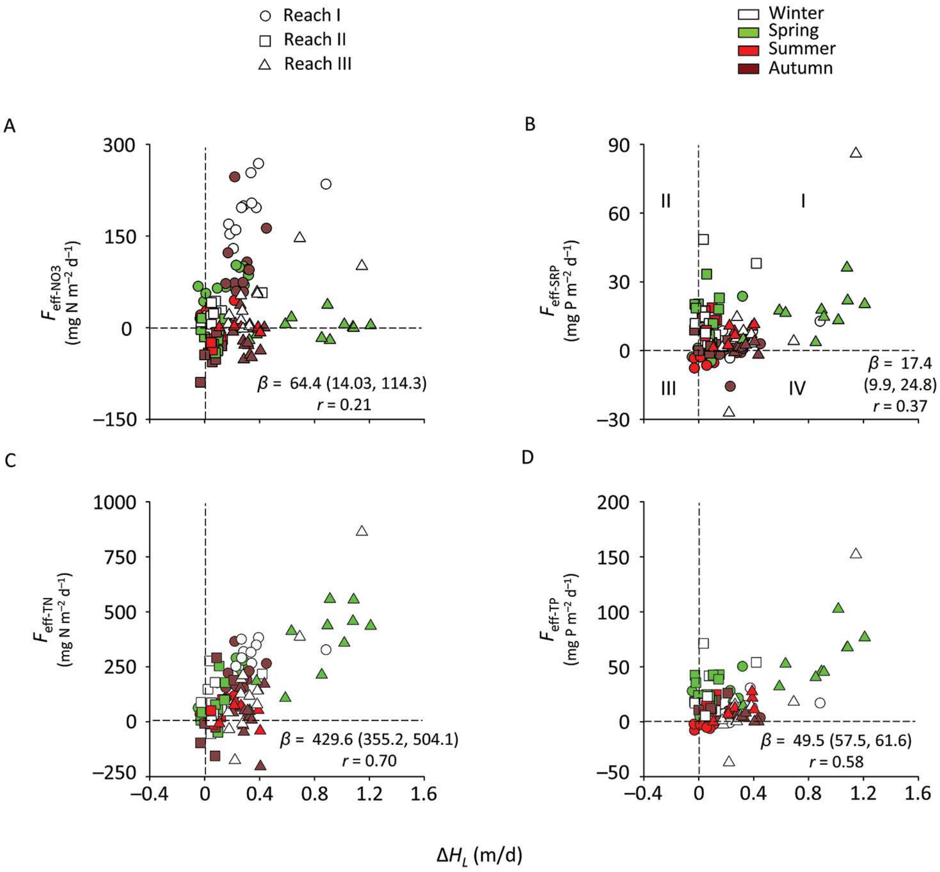

Figure 6. Effective solute flux (F_{eff}, mg m^{-2} d^{-1}) for NO_3-N (A), soluble reactive P (SRP; B), total N (TN; C), and total P (TP; D) vs change in hydraulic load (ΔH_L, m/d) in the Upper Clark Fork River, Montana, USA. Symbols represent back-transformed mean values for individual seasons over the 11-y record. Linear model fit between metrics is presented as the unstandardized slope (β) with 95% CI limits as parenthetical values and standardized slopes (correlation coefficient, *r*). Dashed lines define functional quadrants via negative and positive distinction for each metric. Roman numerals in panel B denote graph quadrants referenced in the text. Similar plots for individual reaches are provided in Figs S4 and S5.

(Fig. 7A, white squares and triangles). Reach III acted as a conduit during both spring and summer before eventually functioning as a consumer during autumn (Fig. 7A, triangles). Reach II, on the other hand, transitioned directly from compiler to consumer during spring with little variation in the exchange effect, followed by enhanced magnitude of load reduction as season progressed from summer to autumn (Fig. 7A, squares).

For SRP, the NPD for a given reach was generally opposite that observed for NO_3^- (Fig. 7B). On an annual basis, reach I was an SRP conduit but extensive depletion, lowest ΔH_L, and robust sink behavior characterized its role as a consumer during summer (Fig. 7B, red circles). During the growing season, reaches II and III were SRP enhancers and compilers, respectively (Fig. 7B), while they simultaneously served as NO_3^- consumers. In the case of TN and TP, reach character was more heavily influenced by ΔH_L than was character for NO_3^- or SRP. Loads increased with greater inflow and little change in concentration (Fig. 7C, D). Reaches behaved mostly as TN and TP compilers but occasionally as enhancers when load increases were related to enrichment (i.e., reach I for TN and reach II for TP).

DISCUSSION

Reaches in functional space: Local and routing influences on reach character

Mass-balance assessment of reaches I, II, and III in the UCFR identified distinct biogeochemical behavior that differed by nutrient, location along the river, and time as seasons progressed from winter through snowmelt into prolonged baseflow conditions during the growing season. In combination, distinct values for NMB, ΔH_L, and availability are a set of biogeochemical traits representative of a given reach that results in it residing within a specific NPD. NPDs, thus, differ as a result of having contrasting dominant fates for solutes, distinguishing retention and removal from transport (Grimm et al. 2003), and having different potential for load alteration to be linked to exchange flows (Bencala 1983, Helton et al. 2011, Stewart et al. 2011). Additionally,

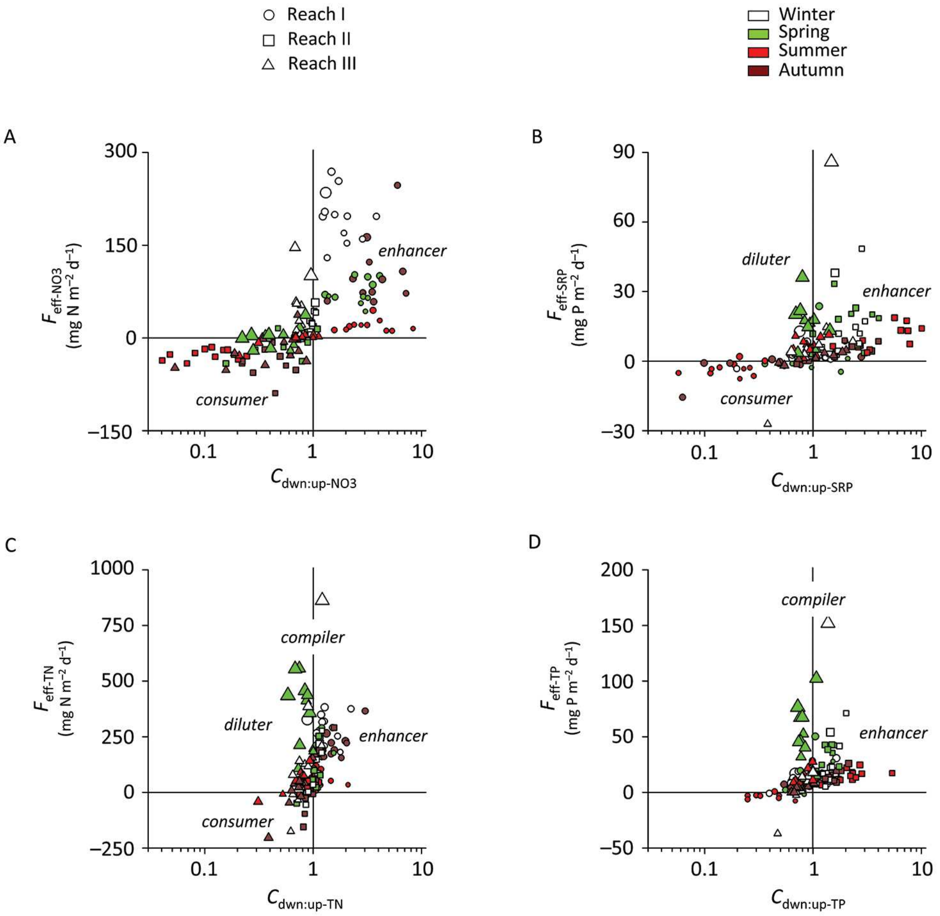

Figure 7. Seasonal patterns of effective solute flux (F_{eff}) and the ratio of downstream-to-upstream concentration ($C_{\text{dwn:up}}$) for NO_3-N (A), soluble reactive P (SRP; B), total N (TN; C), and total P (TP; D) among the 3 study reaches, Upper Clark Fork River, Montana, USA. Data are back-transformed seasonal means for each of the 11 y of record. Lines delineate negative from positive values for F_{eff} and distinguish concentration decrease ($C_{\text{dwn:up}} < 1$) from increase ($C_{\text{dwn:up}} > 1$). Exchange potential is reflected by symbol sizes corresponding to the magnitude of changes in hydraulic load ($\Delta H_L = -0.43$–1.21 m/d; see Fig. 6A–D). Nutrient processing domains (NPDs; diluter, enhancer, consumer, compiler) reflect reach behavior in functional space described by net material balance (NMB) and the availability effect. Solid lines define positions in functional space not different from the null values for availability (conserved concentration, $C_{\text{dwn:up}} = 1$) and NMB (material steady state, $F_{\text{eff}} = 0$). Note the ln-transformed nature of the *x*-axis associated with the availability effect.

some domains are characterized by enrichment, whereas others include reaches characterized by declining nutrient concentrations (i.e., depletion). We contend that the patterns of N and P loading (routing control) and biological uptake (local processes) generate emergent biogeochemical character among reaches that places them in distinct NPDs along the UCFR. The distribution of these reaches results in a biogeochemical discontinuum along the river corridor (Poole 2002), reflecting different biophysical templates and contrasting patterns of nutrient retention and transport at seasonal and annual scales.

NPD patterns and mechanisms

Spatial distribution and seasonal changes in reach processing of NO_3-N illustrate contrasting influences along the UCFR. Throughout the year, reach I acted as a robust NO_3^- enhancer, typically doubled in flow rate, and displayed substantial enrichment, suggesting inflow of N-rich water over its length. By contrast, maximum NO_3-N retention occurred in reach II, where $F_{\text{eff-NO3}}$ was increasingly negative as seasons progressed from spring through autumn (Fig. 4A). In this reach, discharge accumulation was minimal, and $F_{\text{eff-NO3}}$ was unrelated to seasonal changes in stream flow (Fig. S4A). The propensity for reach II to behave as an NO_3^- consumer over annual time frames and during all seasons but winter appears tied to relatively little exogenous transverse load and active biological uptake. Calculated $F_{\text{eff-NO3}}$ values for reaches II and III during the growing season (-1.4 to -60.0 mg N m^{-2} d^{-1}; Fig. 4A) despite unmeasured import of N (i.e., $+\Delta H_L$) were comparable to those determined from nearly 200 tracer studies of N uptake in 1st- to 5th-order streams (-7.5 to -95.0 mg N m^{-2} d^{-1}; calculated from Ensign and Doyle 2006) and net uptake calculated for Walker Branch, Tennessee, USA (up to -79 mg N m^{-2} d^{-1}; from Roberts and Mulholland 2007), and Mississippi River pools (12.6–142.0 79 mg N m^{-2} d^{-1}; calculated from James et al. 2008).

In the UCFR, low NO_3-N concentrations during the growing season (<0.005 mg/L) are associated with blooms of the filamentous green alga (*Cladophora*) in the warm, well-lit, and P-rich waters of the upper reaches (Dodds 1991, Suplee et al. 2012, Banish 2017). Measures of instream gross primary production in these reaches range from 0.4 to 10 g O_2 m^{-2} d^{-1} during summer algal blooms (HMV, unpublished data). Using a stoichiometric approach that assumes algal respiration to be 30% of gross primary production (Meyer 1989), a photosynthetic quotient of 1.0 (Bunn et al. 1999), and molar C:N of 6.6 in algal tissue (Redfield 1958), putative $F_{\text{eff-NO3}}$ values resulting from algal assimilation range from -1.5 to -36.4 mg N m^{-2} d^{-1} and correspond closely with seasonal mean values derived from our mass-balance approach (–1.4 to -60.0 mg N m^{-2} d^{-1}; Fig. 4A–D). Our most negative $F_{\text{eff-NO3}}$ values, however, are outside of this range and occurred during autumn, typically a time of bloom cessation (Banish 2017), when accumulation of detrital organic matter associated with algal decline promotes the potential for near-bed anoxia (HMV, unpublished data). Under these conditions, denitrification may act as an influential NO_3^--removal process (Mulholland et al. 2008), but no measures of this transformation are currently available for the UCFR.

Reach I was a consistent NO_3^- enhancer, but in terms of SRP, its biogeochemical behavior changed with time, associating it with different NPDs as seasons progressed. Although an SRP enhancer during spring, SRP availability was depleted during the growing season as the reach progressed from a source in winter to a consumer during summer (Fig. 4A, B). The juxtaposition of these NPDs suggests exogenous loading of NO_3^- (but not SRP) from the surrounding landscape and increased instream demand for SRP driven by stoichiometric linkage. This perspective is supported by substantial stream flow accumulation (Table 2) and elevated atomic N:P ratios (Table 3) over the course of the reach. Average areal solute flux for summer in reach I (Fig. 4C) were in the lower range of those reported by Ensign and Doyle (2006). At the same time, our net measures derived from mass-balance are expected to be less than those associated with enrichment or isotopic approaches (Martí et al. 1997, Mulholland et al. 2002).

Downstream, reaches II (enhancer) and III (compiler) served as substantial sources of SRP to the river. Throughout the UCFR, SRP concentrations are relatively high (Table 3). While minimum concentrations were consistently observed at the bottom of reach I, much greater concentrations were found in reaches II and III at sites also rich in TP (Table 3). Abundant P in the UCFR, and its loading into reaches II and III, likely reflects interaction between the river network and the geologically P-rich Phosphoria formation that it drains (Carey 1991, Ingman 1992, Knudsen et al. 2002). Historic P mines exist within the mountains draining to reach III via Gold Creek (Carey 1991) near the downstream boundary of the reach (Fig. 2).

Riverine NPDs: Natural and anthropogenic influences on spatial and temporal organization

Our assessment of reach biogeochemical character suggests that exogenous loading and the exchange effect set broad potential for a reach to reside within a given domain, but biogeochemical processing has the capacity to dictate character with potentially equal or greater influence. The occurrence of tributaries or groundwater discharge that provide substantial hydraulic load increases the propensity for reaches to act as compilers or enhancers, but NMB reflects the combined influences of hydrologic and biologic processes that differ in magnitude with solute identity and reactivity. Thus, both spatial distinctions and temporal migrations of net biogeochemical behavior may place reaches into very different NPDs.

For a given reach, seasonal progression among NPDs can be associated with transition from exogenous influences of import during high flow to endogenous processes influential during baseflow. Connections with the surrounding floodplain (Junk et al. 1989, Tockner et al. 2000) or broader contributing network (Hornberger et al. 1994, Mulholland and Hill 1997, Bowes et al. 2014) are maximal during high flow and minimal during baseflow when instream processes may sequester materials and decrease loads (Royer et al. 2006, Mulholland et al. 2008). This is likely the case for the UCFR where concentrations and loads for TN, TP, SRP, and NO_3-N were maximal during winter and spring, when all reaches acted as compilers or enhancers.

The tendency for most reaches to act as TN and TP compilers or enhancers even during low flow, however, is consistent with observations from other river systems where TN and TP loads increase with basin (Smith et al. 2005) or river (Bowes et al. 2003, Duan et al. 2013) size. In general, TN and TP are considered less biologically available than are correspondingly reactive inorganic forms (Bradford and Peters 1987, Hedin et al. 1995, Galloway et al. 2002) and, thus, more prone to conservative behavior and accumulation (Manning et al. 2020). This perspective is congruent with the close relationships between hydrologic gain (i.e., $+\Delta H_L$) and the robust TN and TP load increases we observed for all study reaches (Figs 6, S5).

Instream processes may shift reaches among NPDs. Transitions to consumer behavior during summer and autumn, as observed for NO_3^-, SRP, and TP at different locations in the UCFR, are likely linked to instream uptake by benthic algae. Assimilated nutrients are then typically lost following algal senescence and subsequent export from the reach as particulate organic matter (Grimm 1987, Baulch et al. 2011). Processes within streams may also serve as sources for materials like NO_3^- in systems where the balance among resources favors dissimilatory pathways like nitrification (Bernhardt et al. 2002, Lupon et al. 2020). Stream reaches receiving municipal sewage rich in NH_4-N provide favorable conditions for NO_3^- production and enrichment (Ribot et al. 2012), including the UCFR headwaters (Gammons et al. 2011). In tropical streams, nitrification can represent as much as 39% of NO_3^- export over the river network (Koenig et al. 2017).

A number of cases illustrate that stream reaches may occupy the consumer NPD across an array of stream types. Both survey (Grimm et al. 1981, Dent and Grimm 1999) and budgetary (Grimm 1987, Tate 1990, Martí et al. 1997) approaches to N dynamics in prairie and desert streams illustrate that reaches act as NO_3^- consumers during periods of biomass accrual. Loading of allochthonous organic matter into forested streams can also place reaches within the consumer domain (Mulholland et al. 1985, Valett et al. 2008). Like the patterns observed in reaches II and III in the UCFR, Roberts and Mulholland (2007) showed that Walker Branch transitioned from an NO_3^- source to a consumer during seasonal progression. Bernhardt et al. (2003) showed that import of terrestrial organic matter following a severe ice storm at Hubbard Brook, New Hampshire, USA, resulted in net retention of NO_3^- during summer months. Lupon et al. (2020) documented source and sink behavior for N and C in a boreal headwater stream, with the stream reach acting as consumer for NH_4 and dissolved organic N associated with ecosystem respiration and groundwater influences on instream processes.

For many contemporary systems, the spatial distribution of reaches occupying different NPDs is likely linked to local influences, including both natural and anthropogenic features that differ with location along any given drainage (Poole 2002, Scott et al. 2002). For N and P, increased concentrations and loads along river networks are associated with both point-source and nonpoint-source origins (Carpenter et al. 1998, Wollheim et al. 2008). In particular, point-source discharges create discrete longitudinal changes, generating enhancer reaches with substantive enrichment and little ΔH_L, as illustrated by the influence of sewage inputs to Mediterranean streams (Martí et al. 2004). Other trends appear to reflect cumulative human influences (Smith et al. 2005). Stockner et al. (2000) suggested that large-scale translocation of materials from headwater landscapes to lowlands have enriched larger riverine systems with corresponding cultural oligotrophication of low-order streams. Chronic anthropogenic sources, such as atmospheric deposition (Sullivan et al. 2004, Tabayashi and Koba 2011), agricultural runoff (Park et al. 2018), and urbanization (Sivirichi et al. 2011), increase the spatial complexity of nutrient sources and sinks along the length of rivers systems. More locally, the distribution and composition of riparian vegetation can alter the availability of key, potentially limiting nutrients (Hill 2000, Compton et al. 2003) and the NPDs representative of the reaches associated with them.

Reach boundaries, biogeochemical theory, and distribution among NPDs

To a certain degree, the metabolic and biogeochemical character of a stream reach depends on the delineation of its boundaries (Fisher 1977, Newbold et al. 1982, Hall et al. 2013). Investigation employing the NPD approach may be practically constrained by the co-occurrence of frequent and applicable measures of discharge and concentration (e.g., monitored gauge sites). Theoretically, reach boundaries may be more appropriately associated with abrupt change in the features that impart biogeochemical character (load, concentration, and discharge) reflecting localized transition in net behavior. Investigations can thus be informed by longitudinal assessment of changing nutrient abundance and cumulative flow behaviors and the components of any given drainage system viewed as putative organizers of material transport and retention. In any case, once reaches are established and assessed, the NPD they occupy reflects both internal processes and external linkages, and their longitudinal distribution may provide large-scale constraints on nutrient budgets with implications for river management. For instance, reaches that act as strong consumers may be dependent upon upstream compilers or enhancers. These patterns require understanding of longitudinal organizers of nutrient inputs, their mechanisms of delivery, and their implications for biogeochemical character.

Although some existing models propose the progression of expected metabolic behavior with distance downstream (Vannote et al. 1980, Bernhardt et al. 2018), no similar template has been well developed for stream nutrient concentrations or the longitudinal distribution of expected biogeochemical behavior. Work presented here suggests that longitudinal behavior should emerge from the collective distribution of biogeochemical character and the NPDs that reaches occupy, reflecting both endogenous and exogenous features. Along the world's largest rivers, progression of biogeochemical form and function reflects a myriad of human influences (Best 2019). At the same time, the distribution and intensity of linkage to natural landscape elements, including parent lithology (Valett et al. 1996, Morford et al. 2011), wetlands (Pellerin et al. 2004, Sponseller et al. 2018), lakes (Kling et al. 2000, Jones 2010), and groundwater inputs at multiple scales (Dent et al. 2001, Covino and McGlynn 2007, Peralta-Tapia et al. 2015), likely influence the distribution of sources and sinks (Lupon et al. 2020), suggesting that undisturbed catchments may have historically included distinct consumer and enhancer domains.

NPDs, restoration, and water-quality management

In the context of river restoration and water-quality management, the distribution of reaches among NPDs may strongly influence the efficacy of material retention and productivity. Many restoration practices (e.g., floodplain reconnection, step pools, natural channel design) aim to hydrologically restore streams and rivers with an expectation to decrease nutrient transport (Gabriele et al. 2013, McMillan and Noe 2017). We envision application of the NPD perspective as a valuable asset to set expectations and assess restoration success regarding nutrient retention. In general, the efficacy of restoration practices in regard to measurable change in nutrient retention will vary depending on the biogeochemical character of reaches addressed (i.e., type of NPDs they occupy). Where a restoration goal is to improve water quality by reducing excess nutrients, river restoration activities could prioritize reaches behaving as enhancers or compilers, followed by diluters and conduits, and give minimum priority to consumer reaches, given that they already function as net sinks for materials of concern (Fig. 1). Such ranking of restoration priority is strictly based on the effects that common NPDs have on watershed nutrient export and is likely contrary to the potential for restoration success, given a focus on enhanced water quality. For instance, measurable change in nutrient depletion via channel restoration is unlikely to succeed in reaches acting as strong enhancers, especially when nutrient sources are diffuse and linked to terrestrial origins (e.g., as seen for NO_3^- in reach I). On the other hand, stream channel restoration activities that increase channel width, depth:surface ratio, or water residence time (see Filoso and Palmer 2011) could facilitate transformation of conduits to consumers. Although further examination is surely needed into the potential role of the NPD approach in the toolbox of restoration practitioners and watershed stakeholders, the NPD approach provides a useful functional assessment requiring limited and commonly collected data—concurrent measurements of flow and nutrient concentration at 2 or more locations along a stream network.

Community ecologists interested in species–environment interactions have recently employed a trait-based approach to improve understanding of the mechanisms involved and provide broader generality (Verberk et al. 2013). In many ways, the NPD approach attempts the same sort of trait-based categorization at the ecosystem level of organization. The NPD taxonomy focuses on changes in nutrient loads to define functional units and their traits and tie them to their environmental setting. Understanding the character and distribution of NPD types within the UCFR and other rivers is relevant to a theoretical understanding of how individual reaches function as material reactors, how spatial organization of successive reaches may dictate downstream conditions, and how the balance between local (instream processes) and routing (tributary and upstream loading) determine biogeochemical form and function. At the same time, the NPD concept provides a translatable lexicon and tractable mechanism for incorporating the biogeochemical character of river reaches into approaches aimed at river remediation and restoration.

ACKNOWLEDGEMENTS

Author contributions: The ideas addressed were primarily generated by HMV and other colleagues but fully developed by HMV and MP. HMV and MP collaborated on all aspects of data analysis and interpretation and drafted the manuscript together. GCP improved the quantitative approach and interpretation of results in the 1st draft and assisted HMV and MP in development of the final manuscript.

HMV, MP, and GCP would like to recognize the contribution of many colleagues to idea development associated with the nutrient processing domain concept including Amy Burgin, Steve Hamilton, Kevin McGuire, Ryan Sponseller, Emily Stanley, and Samantha Tappenbeck. The authors appreciate the contributions from the Tri-City Water Council and Dr Mike Suplee at the Montana Department of Environmental Quality for providing the raw data. Support for this effort was derived from the Upper Clark Fork River National Science Foundation (NSF) Long Term Research in Environmental Biology Program (DEB 1655197 to HMV and MP), the Natural Resources Damage Program (Task Order 2.42 to HMV), and the Montana NSF Established Program to Stimulate Competitive Research (Cooperative Agreement OIA-1757351). GCP's participation was supported by the United States Department of Agriculture National Institute of Food and Agriculture, Hatch Project 1015745.

LITERATURE CITED

Abbott, B. W., G. Gruau, J. P. Zarnetske, F. Moatar, L. Barbe, Z. Thomas, O. Fovet, T. Kolbe, S. Gu, A.-C. Pierson-Wickmann, P. Davy, and G. Pinay. 2018. Unexpected spatial stability of water chemistry in headwater stream networks. Ecology Letters 21:296–308.

Aristi, I., M. Arroita, A. Larrañaga, L. Ponsatí, S. Sabater, D. von Schiller, A. Elosegi, and V. Acuña. 2014. Flow regulation by dams affects ecosystem metabolism in Mediterranean rivers. Freshwater Biology 59:1816–1829.

Asano, Y., T. Uchida, Y. Mimasu, and N. Ohte. 2009. Spatial patterns of stream solute concentrations in a steep mountainous catchment with a homogeneous landscape. Water Resources Research 45:WR007466.

Banish, N. J. 2017. Factors influencing Cladophora biomass abundance in the Upper Clark Fork River, Montana. MS Thesis. University of Montana, Missoula, Montana.

Baulch, H. M., E. H. Stanley, and E. S. Bernhardt. 2011. Can algal uptake stop NO_3^- pollution? Nature 477:E3.

Bencala, K. E. 1983. Simulation of solute transportation in a mountain pool-and-riffle stream with kinetic mass transfer model for sorption. Water Resources Research 19:732–738.

Bernhardt, E. S., R. O. Hall Jr, and G. E. Likens. 2002. Whole-system estimates of nitrification and nitrate uptake in streams of the Hubbard Brook Experimental Forest. Ecosystems 5:419–430.

Bernhardt, E. S., J. B. Heffernan, N. B. Grimm, E. H. Stanley, J. W. Harvey, M. Arroita, A. P. Appling, M. J. Cohen, W. H. McDowell, R. O. Hall Jr, J. S. Read, B. J. Roberts, E. G. Stets, and C. B. Yackulic. 2018. The metabolic regimes of flowing waters. Limnology and Oceanography 63:S99–S118.

Bernhardt, E. S., G. E. Likens, D. C. Buso, and C. T. Driscoll. 2003. In-stream uptake dampens effects of major forest disturbance on watershed nitrogen export. Proceedings of the National Academy of Sciences 100:10,304–10,308.

Best, J. 2019. Anthropogenic stresses on the world's big rivers. Nature Geoscience 12:7–21.

Bowes, M. J., W. A. House, and R. A. Hodgkinson. 2003. Phosphorus dynamics along a river continuum. Science of the Total Environment 313:199–212.

Bowes, M. J., H. P. Jarvie, P. S. Naden, G. H. Old, P. M. Scarlett, C. Roberts, L. K. Armstrong, S. A. Harman, H. D. Wickham, and A. L. Collins. 2014. Identifying priorities for nutrient mitigation using river concentration–flow relationships: The Thames basin, UK. Journal of Hydrology 517:1–12.

Bradford, M. E., and R. H. Peters. 1987. The relationship between chemically analyzed phosphorus fractions and bioavailable phosphorus. Limnology and Oceanography 32:1124–1137.

Brinson, M. M. 1993. A hydrogeomorphic classification for wetlands. Wetlands Research Program Technical Report WRP-DE-4. United States Army Corps of Engineers, Waterways Experiment Station, Vicksburg, Mississippi. (Available from: https://wetlands.el.erdc.dren.mil/pdfs/wrpde4.pdf)

Bunn, S. E., P. M. Davies, and T. D. Mosisch. 1999. Ecosystem measures of river health and their response to riparian and catchment degradation. Freshwater Biology 41:333–345.

Burchsted, D., M. Daniels, and E. E. Wohl. 2014. Introduction to the special issue on discontinuity of fluvial systems. Geomorphology 205:1–4.

Burns, D. A. 1998. Retention of NO_3^- in an upland stream environment: A mass balance approach. Biogeochemistry 40:73–96.

Carey, J. H. 1991. Phosphorus sources in Gold Creek, a tributary of the Clark Fork River in western Montana. MS Thesis. University of Montana, Missoula, Montana.

Carpenter, S. R., N. F. Caraco, D. L. Correll, R. W. Howarth, A. N. Sharpley, and V. H. Smith. 1998. Nonpoint pollution of surface waters with phosphorus and nitrogen. Ecological Applications 8:559–568.

Compton, J. E., M. Robbins Church, S. T. Larned, and W. E. Hogsett. 2003. Nitrogen export from forested watersheds in the Oregon Coast range: The role of N_2-fixing red alder. Ecosystems 6:773–785.

Covino, T. P., and B. L. McGlynn. 2007. Stream gains and losses across a mountain-to-valley transition: Impacts on watershed hydrology and stream water chemistry. Water Resources Research 43:WR005544.

Covino, T. P., B. L. McGlynn, and R. A. McNamara. 2010. Tracer Additions for Spiraling Curve Characterization (TASCC): Quantifying stream nutrient uptake kinetics from ambient to saturation. Limnology and Oceanography: Methods 8:484–498.

Creed, I. F., D. M. McKnight, B. A. Pellerin, M. B. Green, B. A. Bergamaschi, G. R. Aiken, D. A. Burns, S. E. G. Findlay, J. B. Shanley, R. G. Striegl, B. T. Aulenbach, D. W. Clow, H. Laudon, B. L. McGlynn, K. J. McGuire, R. A. Smith, and S. M. Stackpoole. 2015. The river as a chemostat: Fresh perspectives on dissolved organic matter flowing down the river continuum. Canadian Journal of Fisheries and Aquatic Sciences 72:1272–1285.

Dent, C. L., and N. B. Grimm. 1999. Spatial heterogeneity of stream water nutrient concentrations over successional time. Ecology 80:2283–2298.

Dent, C. L., N. B. Grimm, and S. G. Fisher. 2001. Multi-scale effects of surface-subsurface exchange on stream water nutrient concentrations. Journal of the North American Benthological Society 20:162–181.

Dodds, W. K. 1991. Factors associated with dominance of the filamentous green-alga *Cladophora glomerata*. Water Research 25:1325–1332.

Dodds, W. K., V. H. Smith, and B. Zander. 1997. Developing nutrient targets to control benthic chlorophyll levels in streams: A case study of the Clark Fork River. Water Research 31: 1738–1750.

Duan, W., K. Takara, B. He, P. Luo, D. Nover, and Y. Yamashiki. 2013. Spatial and temporal trends in estimates of nutrient and suspended sediment loads in the Ishikari River, Japan, 1985 to 2010. Science of the Total Environment 461–462:499–508.

Ensign, S. H., and M. W. Doyle. 2006. Nutrient spiraling in streams and river networks. Journal of Geophysical Research: Biogeosciences 111:JG000114.

Filoso, S., and M. A. Palmer. 2011. Assessing stream restoration effectiveness at reducing nitrogen export to downstream waters. Ecological Applications 21:1989–2006.

Fisher, S. G. 1977. Organic matter processing by a stream-segment ecosystem: Fort River, Massachusetts, U.S.A. Internationale Revue der gesamten Hydrobiologie 62:701–727.

Fisher, S. G., L. G. Gray, N. B. Grimm, and D. E. Busch. 1982. Temporal succession in a desert stream ecosystem following flash flooding. Ecological Monographs 43:421–439.

Freixa, A., E. Ejarque, S. Crognale, S. Amalfitano, S. Fazi, A. Butturini, and A. M. Romaní. 2016. Sediment microbial communities rely on different dissolved organic matter sources along a Mediterranean river continuum. Limnology and Oceanography 61:1389–1405.

Gabriele, W., N. Welti, and T. Hein. 2013. Limitations of stream restoration for nitrogen retention in agricultural headwater streams. Ecological Engineering 60:224–234.

Galloway, J. N., E. B. Cowling, S. P. Seitzinger, and R. H. Socolow. 2002. Reactive nitrogen: Too much of a good thing? Ambio 31: 60–63.

Gammons, C. H., J. N. Babcock, S. R. Parker, and S. R. Poulson. 2011. Diel cycling and stable isotopes of dissolved oxygen, dissolved inorganic carbon, and nitrogenous species in a stream receiving treated municipal sewage. Chemical Geology 283:44–55.

Gibert, J., P. Vervier, F. Malard, R. Laurent, and J.-L. Reygrobellet. 1994. Dynamics of communities and ecology of karst ecosystems: Example of three karsts in eastern and southern France. Pages 425–450 *in* J. Gibert, D. Danielopol, and J. A. Standford (editors). Ground water ecology. Academic Press, San Diego, California.

Gregory, S. V., F. J. Swanson, W. A. McKee, and K. W. Cummins. 1991. An ecosystem perspective of riparian zones: Focus on links between land and water. BioScience 41:540–551.

Grenouillet, G., D. Pont, and C. Hérissé. 2004. Within-basin fish assemblage structure: The relative influence of habitat versus stream spatial position on local species richness. Canadian Journal of Fisheries and Aquatic Sciences 61:93–102.

Grimm, N. B. 1987. Nitrogen dynamics during succession in a desert stream. Ecology 68:1157–1170.

Grimm, N. B., S. G. Fisher, and W. L. Minckley. 1981. Nitrogen and phosphorus dynamics in hot desert streams of Southwestern USA. Hydrobiologia 83:303–312.

Grimm, N. B., S. E. Gergel, W. H. McDowell, E. W. Boyer, C. L. Dent, P. Groffman, S. C. Hart, J. Harvey, C. Johnston, and E. Mayorga. 2003. Merging aquatic and terrestrial perspectives of nutrient biogeochemistry. Oecologia 137:485–501.

Hall Jr, R. O., M. A. Baker, E. J. Rosi-Marshall, J. L. Tank, and J. D. Newbold. 2013. Solute-specific scaling of inorganic nitrogen and phosphorus uptake in streams. Biogeosciences 10:7323–7331.

Harvey, J. W., and B. J. Wagner. 2000. Quantifying hydrologic interactions between streams and their subsurface hyporheic zones. Pages 3–44 in J. B. Jones and P. J. Mulholland (editors). Streams and ground waters. Academic Press, San Diego, California.

Hedin, L. O., J. J. Armesto, and A. H. Johnson. 1995. Patterns of nutrient loss from unpolluted, old-growth temperate forests: Evaluation of biogeochemical theory. Ecology 76:493–509.

Helton, A. M., G. C. Poole, J. L. Meyer, W. M. Wollheim, B. J. Peterson, P. J. Mulholland, E. S. Bernhardt, J. A. Stanford, C. Arango, L. R. Ashkenas, L. W. Cooper, W. K. Dodds, S. V. Gregory, R. O. Hall Jr, S. K. Hamilton, S. L. Johnson, W. H. McDowell, J. D. Potter, J. L. Tank, S. M. Thomas, H. M. Valett, J. R. Webster, and L. Zeglin. 2011. Thinking outside the channel: Modeling nitrogen cycling in networked river ecosystems. Frontiers in Ecology and the Environment 9:229–238.

Hill, A. R. 2000. Stream chemistry and riparian zones. Pages 83–1110 in J. B. Jones and P. J. Mulholland (editors). Streams and ground waters. Academic Press, San Diego, California.

Hornberger, G. M., K. E. Bencala, and D. M. McKnight. 1994. Hydrological controls on dissolved organic carbon during snowmelt in the Snake River near Montezuma, Colorado. Biogeochemistry 25:147–165.

Houser, J. N., P. J. Mulholland, and K. O. Maloney. 2005. Catchment disturbance and stream metabolism: Patterns in ecosystem respiration and gross primary production along a gradient of upland soil and vegetation disturbance. Journal of the North American Benthological Society 24:538–552.

Humphries, P., H. Keckeis, and B. Finlayson. 2014. The River Wave Concept: Integrating river ecosystem models. BioScience 64:870–882.

Hurlbert, S. H. 1984. Pseudoreplication and the design of ecological field experiments. Ecological Monographs 54:187–211.

Ingman, G. L. 1992. Assessment of phosphorus and nitrogen sources in the Clark Fork River Basin, 1988–1991: Final report. Montana Department of Health and Environmental Services, Water Quality Bureau, Helena, Montana.

James, W. F., W. B. Richardson, and D. M. Soballe. 2008. Contribution of sediment fluxes and transformations to the summer nitrogen budget of an Upper Mississippi River backwater system. Hydrobiologia 598:95–107.

Jencso, K. G., B. L. McGlynn, M. N. Gooseff, S. M. Wondzell, K. E. Bencala, and L. A. Marshall. 2009. Hydrologic connectivity between landscapes and streams: Transferring reach- and plot-scale understanding to the catchment scale. Water Resources Research 45:WR007225.

Jones, N. E. 2010. Incorporating lakes within the river discontinuum: Longitudinal changes in ecological characteristics in stream–lake networks. Canadian Journal of Fisheries and Aquatic Sciences 67:1350–1362.

Junk, W. J., P. B. Bayley, and R. E. Sparks. 1989. The flood pulse concept in river-floodplain systems. Canadian Special Publications in Fisheries and Aquatic Science 106:110–127.

Kadlec, R. H., and S. D. Wallace. 2009. Treatment wetlands. 2nd edition. CRC Press, New York, New York.

Kling, G. W., G. W. Kipphut, M. M. Miller, and W. J. O'Brien. 2000. Integration of lakes and streams in a landscape perspective: The importance of material processing on spatial patterns and temporal coherence. Freshwater Biology 43:477–497.

Knudsen, A. C., M. E. Gunter, J. R. Herring, and R. I. Grauch. 2002. Mineralogical characterization of weathered and less weathered strata of the Meade Peak phosphatic shale member of the Permian Phosphoria Formation; measured sections E and F, Rasmussen Ridge, and measured sections G and H, Sage Creek area of the Webster Range, Caribou County, Idaho. Open-File Report 02-392. United States Geological Survey. (Available from: https://pubs.usgs.gov/of/2002/0392/)

Koenig, L. E., C. Song, W. M. Wollheim, J. Rüegg, and W. H. McDowell. 2017. Nitrification increases nitrogen export from a tropical river network. Freshwater Science 36:698–712.

Lupon, A., B. A. Denfeld, H. Laudon, J. Leach, and R. A. Sponseller. 2020. Discrete groundwater inflows influence patterns of nitrogen uptake in a boreal headwater stream. Freshwater Science 39:228–240.

Mallard, J., B. McGlynn, and T. Covino. 2014. Lateral inflows, stream-groundwater exchange, and network geometry influence stream water composition. Water Resources Research 50:4603–4623.

Manning, D. W. P., A. D. Rosemond, J. P. Benstead, P. M. Bumpers, and J. S. Kominoski. 2020. Transport of N and P in U.S. streams and rivers differs with land use and between dissolved and particulate forms. Ecological Applications 30:e02130.

Martí, E., J. Aumatell, L. Godé, M. Poch, and F. Sabater. 2004. Nutrient retention efficiency in streams receiving inputs from wastewater treatment plants. Journal of Environmental Quality 33:285–293.

Martí, E., N. B. Grimm, and S. G. Fisher. 1997. Pre- and post-flood retention efficiency of nitrogen in a Sonoran Desert stream. Journal of the North American Benthological Society 16:805–819.

McGuire, K. J., C. E. Torgersen, G. E. Likens, D. C. Buso, W. H. Lowe, and S. W. Bailey. 2014. Network analysis reveals multiscale controls on streamwater chemistry. Proceedings of the National Academy of Sciences 111:7030–7035.

McMillan, S. K., and G. B. Noe. 2017. Increasing floodplain connectivity through urban stream restoration increases nutrient and sediment retention. Ecological Engineering 108:284–295.

McTammany, M. E., J. R. Webster, E. F. Benfield, and M. A. Neatrour. 2003. Longitudinal patterns of metabolism in a southern Appalachian river. Journal of the North American Benthological Society 22:359–370.

Meyer, J. L. 1989. Can P/R ratio be used to assess the food base of stream ecosystems? A comment on Rosenfeld and Mackay (1987). Oikos 54:119–121.

Minshall, G. W., D. A. Andrews, and C. Y. Manuel-Faler. 1983. Application of Island Biogeographic Theory to streams: Macroinvertebrate recolonization of the Teton River, Idaho. Pages 279–297 in J. R. Barnes and G. W. Minshall (editors). Stream ecology: Application and testing of general ecological theory. Plenum Press, New York, New York.

Molles Jr, M. C. 1982. Trichopteran communities of streams associated with aspen and conifer forests: Long-term structural change. Ecology 63:1–6.

Montana Department of Justice. 2012. Final Upper Clark Fork River Basin aquatic and terrestrial resources restoration plans. Natural Resources Damage Program, Helena, Montana. (Available from: https://dojmt.gov/wp-content/uploads/Final-AT-Restoration-Plan-Combined.pdf)

Montgomery, D. R. 1999. Process domains and the river continuum. Journal of the American Water Resources Association 35:397–410.

Moore, J. N., E. Brook, and C. Johns. 1989. Grain size partitioning of metals in contaminated, coarse-grained river floodplain sediment: Clark Fork River, Montana, U.S.A. Environmental Geology and Water Sciences 14:107–115.

Moore, J. N., and H. W. Langner. 2012. Can a river heal itself? Natural attenuation of metal contamination in river sediment. Environmental Science & Technology 46:2616–2623.

Morford, S. L., B. Z. Houlton, and R. A. Dahlgren. 2011. Increased forest ecosystem carbon and nitrogen storage from nitrogen rich bedrock. Nature 477:78–81.

Mulholland, P. J., A. M. Helton, G. C. Poole, R. O. Hall, S. K. Hamilton, B. J. Peterson, J. L. Tank, L. R. Ashkenas, L. W. Cooper, C. N. Dahm, W. K. Dodds, S. E. G. Findlay, S. V. Gregory, N. B. Grimm, S. L. Johnson, W. H. McDowell, J. L. Meyer, H. M. Valett, J. R. Webster, C. P. Arango, J. J. Beaulieu, M. J. Bernot, A. J. Burgin, C. L. Crenshaw, L. T. Johnson, B. R. Niederlehner, J. M. O'Brien, J. D. Potter, R. W. Sheibley, D. J. Sobota, and S. M. Thomas. 2008. Stream denitrification across biomes and its response to anthropogenic nitrate loading. Nature 452:202–205.

Mulholland, P. J., and W. R. Hill. 1997. Seasonal patterns in streamwater nutrient and dissolved organic carbon concentrations: Separating catchment flow path and in-stream effects. Water Resources Research 33:1297–1306.

Mulholland, P. J., J. D. Newbold, J. W. Elwood, L. A. Ferren, and J. R. Webster. 1985. Phosphorus spiraling in a woodland stream: Seasonal variations. Ecology 66:1012–1023.

Mulholland, P. J., J. L. Tank, J. R. Webster, W. B. Bowden, W. K. Dodds, S. V. Gregory, N. B. Grimm, S. K. Hamilton, S. L. Johnson, E. Martí, W. H. McDowell, J. L. Merriam, J. L. Meyer, B. J. Peterson, H. M. Valett, and W. M. Wollheim. 2002. Can uptake length be determined by nutrient addition experiments? Results from an interbiome study. Journal of the North American Benthological Society 21:544–560.

Munn, N. L., and J. L. Meyer. 1990. Habitat-specific solute retention in two small streams: An intersite comparison. Ecology 71:2069–2082.

Newbold, J. D. 1992. Cycles and spirals of nutrients. Pages 379–399 *in* P. Calow and G. E. Petts (editors). The rivers handbook. Blackwell Scientific Publications, Oxford, United Kingdom.

Newbold, J. D., P. J. Mulholland, J. W. Elwood, and R. V. O'Neill. 1982. Organic carbon spiralling in stream ecosystems. Oikos 38:266–272.

Nimick, D. A., and J. N. Moore. 1993. Stratigraphy and chemistry of sulfidic flood-plain sediments in the Upper Clark Fork Valley, Montana. Pages 276–288 *in* C. N. Alpers and D. W. Blowes (editors). Environmental geochemistry of sulfide oxidation. American Chemical Society, Washington, DC.

Park, Y., Y. Kim, S.-K. Park, W.-J. Shin, and K.-S. Lee. 2018. Water quality impacts of irrigation return flow on stream and groundwater in an intensive agricultural watershed. Science of the Total Environment 630:859–868.

Peipoch, M., E. Gacia, E. Bastias, A. Serra, L. Proia, M. Ribot, S. Merbt, and E. Martí. 2016. Small-scale heterogeneity of microbial N uptake in streams and its implications at the ecosystem level. Ecology 97:1329–1344.

Pellerin, B., W. Wollheim, C. Hopkinson, W. McDowell, M. Williams, C. Vörösmarty, and M. Daley. 2004. Role of wetlands and developed land use on dissolved organic nitrogen concentrations and DON/TDN in Northeastern U.S. rivers and streams. Limnology and Oceanography 49:910–918.

Peralta-Tapia, A., R. A. Sponseller, A. Ågren, D. Tetzlaff, C. Soulsby, and H. Laudon. 2015. Scale-dependent groundwater contributions influence patterns of winter baseflow stream chemistry in boreal catchments. Journal of Geophysical Research: Biogeosciences 120:847–858.

Peterson, B. J., W. M. Wollheim, P. J. Mulholland, J. R. Webster, J. L. Meyer, J. L. Tank, E. Martí, W. B. Bowden, H. M. Valett, A. E. Hershey, W. H. McDowell, W. K. Dodds, S. K. Hamilton, S. Gregory, and D. D. Morrall. 2001. Control of nitrogen export from watersheds by headwater streams. Science 292:86–90.

Poole, G. C. 2002. Fluvial landscape ecology: Addressing uniqueness within the river discontiuum. Freshwater Ecology 47:641–660.

Redfield, A. C. 1958. The biological control of chemical factors in the environment. American Scientist 46:205–221.

Ribot, M., E. Martí, D. von Schiller, F. Sabater, H. Daims, and T. J. Battin. 2012. Nitrogen processing and the role of epilithic biofilms downstream of a wastewater treatment plant. Freshwater Science 31:1057–1069.

Rich, C. F., T. E. McMahon, B. E. Rieman, and W. L. Thompson. 2003. Local-habitat, watershed, and biotic features associated with Bull Trout occurrence in Montana streams. Transactions of the American Fisheries Society 132:1053–1064.

Roberts, B. J., and P. J. Mulholland. 2007. In-stream biotic control on nutrient biogeochemistry in a forested stream, West Fork of Walker Branch. Journal of Geophysical Research: Biogeosciences 112:JG000422.

Rosenfeld, J. S., J. Post, G. Robins, and T. Hatfield. 2007. Hydraulic geometry as a physical template for the River Continuum: Application to optimal flows and longitudinal trends in salmonid habitat. Canadian Journal of Fisheries and Aquatic Sciences 64:755–767.

Royer, T. V., M. B. David, and L. E. Gentry. 2006. Timing of riverine export of nitrate and phosphorus from agricultural watersheds in Illinois: Implications for reducing nutrient loading to the Mississippi River. Environmental Science & Technology 40:4126–4131.

Schade, J. D., S. G. Fisher, N. B. Grimm, and J. A. Seddon. 2001. The influence of a riparian shrub on nitrogen cycling in a Sonoran Desert stream. Ecology 82:3363–3376.

Scott, M. C., G. S. Helfman, M. E. McTammany, E. F. Benfield, and P. Bolstad. 2002. Multiscale influences on physical and chemical stream conditions across Blue Ridge landscapes. Journal of the American Water Resources Association 38:1379–1392.

Sivirichi, G. M., S. S. Kaushal, P. Mayer, C. Welty, K. T. Belt, T. A. Newcomer, K. D. Newcomb, and M. M. Grese. 2011. Longitudinal variability in streamwater chemistry and carbon and nitrogen fluxes in restored and degraded urban stream networks. Journal of Environmental Monitoring 13:288–303.

Smith, S. V., D. P. Swaney, R. W. Buddemeier, M. R. Scarsbrook, M. A. Weatherhead, C. Humborg, H. Eriksson, and F. Hannerz. 2005. River nutrient loads and catchment size. Biogeochemistry 75:83–107.

Sponseller, R. A., M. Blackburn, M. B. Nilsson, and H. Laudon. 2018. Headwater mires constitute a major source of nitrogen (N) to surface waters in the Boreal landscape. Ecosystems 21:31–44.

Stewart, R. J., W. M. Wollheim, M. Gooseff, M. A. Briggs, J. M. Jacobs, B. J. Peterson, and C. S. Hopkinson. 2011. Separation of river network scale nitrogen removal among main channel and two transient storage compartments. Water Resources Research 47:W00J10.

Stockner, J. G., E. Rydin, and P. Hyenstrand. 2000. Cultural oligotrophication: Causes and consequences for fisheries resources. Fisheries 25(5):7–14.

Stream Solute Workshop. 1990. Concepts and methods for assessing solute dynamics in stream ecosystems. Journal of the North American Benthological Society 9:95–119.

Sullivan, T. J., B. J. Cosby, A. T. Herlihy, J. R. Webb, A. J. Bulger, K. U. Snyder, P. F. Brewer, E. H. Gilbert, and D. L. Moore. 2004. Regional model projections of future effects of sulfur and nitrogen deposition on streams in the southern Appalachian Mountains. Water Resources Research 40:WR001998.

Suplee, M. W., A. Varghese, and J. Cleland. 2007. Developing nutrient criteria for streams: An evaluation of the frequency distribution method. Journal of the American Water Resources Association 43:453–472.

Suplee, M. W., V. Watson, W. K. Dodds, and C. Shirley. 2012. Response of algal biomass to large-scale controls in the Clark Fork River, Montana, United States. Journal of the American Water Resources Association 48:1008–1021.

Tabayashi, Y., and K. Koba. 2011. Heterogeneous atmospheric nitrogen deposition effects upon the nitrate concentration of stream waters in a forested mountain area. Water, Air, & Soil Pollution 216:105–115.

Tank, J. L., E. Martí, T. Riis, D. von Schiller, A. J. Reisinger, W. K. Dodds, M. R. Whiles, L. R. Ashkenas, W. B. Bowden, S. M. Collins, C. L. Crenshaw, T. A. Crowl, N. A. Griffiths, N. B. Grimm, S. K. Hamilton, S. L. Johnson, W. H. McDowell, B. M. Norman, E. J. Rosi, K. S. Simon, S. A. Thomas, and J. R. Webster. 2018. Partitioning assimilatory nitrogen uptake in streams: An analysis of stable isotope tracer additions across continents. Ecological Monographs 88:120–138.

Tate, C. M. 1990. Patterns and controls of nitrogen in tallgrass prairie streams. Ecology 71:2007–2018.

Thorp, J. H., M. C. Thoms, and M. D. Delong. 2006. The riverine ecosystem synthesis: Biocomplexity in river networks across space and time. River Research and Applications 22:123–147.

Tiwari, T., I. Buffam, R. A. Sponseller, and H. Laudon. 2017. Inferring scale-dependent processes influencing stream water biogeochemistry from headwater to sea. Limnology and Oceanography 62:S58–S70.

Tockner, K., F. Malard, and J. V. Ward. 2000. An extension of the flood pulse concept. Hydrological Processes 14:2861–2883.

Townsend, C. R. 1989. The patch dynamics concept of stream community ecology. Journal of the North American Benthological Society 8:36–50.

Tri-State Water Council. 2009. The Clark Fork River Voluntary Nutrient Reduction Program 1998–2008. The progress of a voluntary program in reducing nutrients and noxious algae in the Clark Fork River in Montana. Tri-State Implementation Council, Sandpoint, Idaho.

Valett, H. M., F. R. Hauer, and J. A. Stanford. 2014. Landscape influences on ecosystem function: Local and routing control of oxygen dynamics in a floodplain aquifer. Ecosystems 17:195–211.

Valett, H. M., J. A. Morrice, C. N. Dahm, and M. E. Campana. 1996. Parent lithology, surface–groundwater exchange, and nitrate retention in headwater streams. Limnology and Oceanography 41: 333–345.

Valett, H. M., S. A. Thomas, P. J. Mulholland, J. R. Webster, C. N. Dahm, C. S. Fellows, C. L. Crenshaw, and C. G. Peterson. 2008. Endogenous and exogenous control of nitrate uptake in headwater streams. Ecology 89:3515–3527.

Vannote, R. L., G. W. Minshall, K. W. Cummins, J. R. Sedell, and C. E. Cushing. 1980. The River Continuum Concept. Canadian Journal of Fisheries and Aquatic Sciences 37:130–137.

Verberk, W. C. E. P., C. G. E. van Noordwijk, and A. G. Hildrew. 2013. Delivering on a promise: Integrating species traits to transform descriptive community ecology into a predictive science. Freshwater Science 32:531–547.

Watson, V. 1989. Maximum levels of attached algae in the Clark Fork River. Proceedings of the Montana Academy of Sciences 49:27–35.

Webster, J. R., J. D. Newbold, S. A. Thomas, H. M. Valett, and P. J. Mulholland. 2009. Nutrient uptake and mineralization during leaf decay in streams—A model simulation. International Review of Hydrobiology 94:372–390.

Webster, J. R., and H. M. Valett. 2007. Solute dynamics. Pages 169–186 in F. R. Hauer and G. A. Lamberti (editors). Methods in stream ecology: Field and laboratory exercises. Academic Press, San Diego, California.

Williams, M. W., and J. M. Melack. 1991. Solute chemistry of snowmelt and runoff in an Alpine Basin, Sierra Nevada. Water Resources Research 27:1575–1588.

Wollheim, W. M., B. J. Peterson, S. M. Thomas, C. H. Hopkinson, and C. J. Vörösmarty. 2008. Dynamics of N removal over annual time periods in a suburban river network. Journal of Geophysical Research: Biogeosciences 113:JG000660.